sustainability

MDPI

Article

Assessment of Weather Research and Forecasting (WRF) Physical Schemes Parameterization to Predict Moderate to Extreme Rainfall in Poorly Gauged Basin

Syeda Maria Zaidi [1,2,*], Jacqueline Isabella Anak Gisen [1,3,*], Mohamed Eltahan [4,5], Qian Yu [3,6], Syarifuddin Misbari [1] and Su Kong Ngien [1]

1 Faculty of Civil Engineering Technology, Universiti Malaysia Pahang, Lebuh Persiaran Tun Khalil Yaakob, Kuantan 26300, Pahang, Malaysia
2 Civil Engineering Department, Balochistan University of Engineering and Technology, Khuzdar 89100, Balochistan, Pakistan
3 State Key Laboratory of Simulation and Regulation of Water Cycle in River Basin, China Institute of Water Resources and Hydropower Research, Beijing 100038, China
4 Institute of Geosciences, Division of Meteorology, University of Bonn, 53121 Bonn, Germany
5 Institute of Bio- and Geosciences (Agrosphere, IBG-3), Research Centre Jülich, 52428 Jülich, Germany
6 Research Center on Flood and Drought Disaster Reduction of the Ministry of Water Resources, Beijing 100038, China
* Correspondence: maria.zaidi@buetk.edu.pk (S.M.Z.); isabella@ump.edu.my (J.I.A.G.)

Abstract: Incomplete hydro-meteorological data and insufficient rainfall gauges have caused difficulties in establishing a reliable flood forecasting system. This study attempted to adopt the remotely sensed hydro-meteorological data as an alternative to the incomplete observed rainfall data in the poorly gauged Kuantan River Basin (KRB), the main city at the east coast of Peninsula Malaysia. Performance of Weather Research and Forecasting (WRF) schemes' combinations, including eight microphysics (MP) and six cumulus, were evaluated to determine the most suitable combination of WRF MPCU in simulating rainfall over KRB. All the obtained results were validated against observed moderate to extreme rainfall events. Among all, the combination scheme Stony Brook University and Betts–Miller–Janjic (SBUBMJ) was found to be the most suitable to capture both spatial and temporal rainfall, with average percentage error of about ±17.5% to ±25.2% for heavy and moderate rainfall. However, the estimated PE ranges of −58.1% to 68.2% resulted in uncertainty while simulating extreme rainfall events, requiring more simulation tests for the schemes' combinations using different boundary layer conditions and domain configurations. Findings also indicate that for the region where hydro-meteorological data are limited, WRF, as an alternative approach, can be used to achieve more sustainable water resource management and reliable hydrological forecasting.

Keywords: WRF; microphysics scheme; cumulus scheme; floods; rainfall

Citation: Zaidi, S.M.; Gisen, J.I.A.; Eltahan, M.; Yu, Q.; Misbari, S.; Ngien, S.K. Assessment of Weather Research and Forecasting (WRF) Physical Schemes Parameterization to Predict Moderate to Extreme Rainfall in Poorly Gauged Basin. *Sustainability* **2022**, *14*, 12624. https://doi.org/10.3390/su141912624

Academic Editors: Sungwon Kim and Salim Heddam

Received: 29 July 2022
Accepted: 27 September 2022
Published: 4 October 2022

1. Introduction

The ability to accurately estimate rainfall has significant importance in theoretical as well as practical amplification [1]. Moreover, timely and accurate prediction of rainfall at the regional and global levels is highly important for making preventive measurements for flood management [2,3]. Effective forecasting is primarily dependent on the accuracy of the numerical model to determine the intensity, spatial, and temporal pattern of precipitation at both global and regional levels. In general, rain is the more challenging variable to be forecasted [4]. There have been several studies that applied global models to analyze the process of large-scale atmospheric circulation and quantify the rainfall events. However, they are unable to capture accurate rainfall events due to their coarse resolution [5–9]. Numerical weather prediction at the regional level, on the other hand, can properly simulate

large-scale weather phenomena, resulting in better representation of convection. For this reason, regional models are increasingly being used to investigate rainfall scenarios [10–12].

Although the quantification of rainfall employing numerical models is a complex process, the regional level scale Fifth-Generation Penn State/NCAR Mesoscale Model (MM5) and Weather Research and Forecasting (WRF) model are frequently used and popular for operational forecasting concerning their performance. The advance research Weather Research and Forecasting (WRF) model is the most recent popular community model that has been extensively used in several applications related to meteorological phenomena such as rainfall and thunderstorms [13,14]. According to studies, the WRF model can produce high-resolution spatial and temporal rainfall simulation results, indicating that the WRF model can increase runoff simulation accuracy for flood disaster prevention [15,16]. Several forecasting reviews have been conducted by the WRF user community to evaluate WRF's performance in a variety of forecasting applications [14,17,18]. Refs. [19,20] have further confirmed the WRF model's ability to provide significant values to represent the convective system and efficiently identify tornadic and non-tornadic events using predictable initial data with high grid resolution. Ref. [21] evaluated the effectiveness of the WRF microphysical scheme to investigate the latent heat ratio associated with the mesoscale convective system and to simulate the distribution pattern of convective rainfall over the Korean Peninsula. The 36-grid km WRF model has been found to be capable of producing accurate one-day monsoon forecasts for the Indian region [22].

Many studies explored the parameterization of multiple physical schemes available in the WRF model for simulating rainfall events, such as the microphysics (MP) scheme [23–25], cumulus (CU) parameterization scheme [26,27], land surface model (LSM) options [28–30], and planetary boundary layer (PBL) scheme [31,32]. The study [33] conducted on Mumbai, India's west coast discovered that parameterizing MP WRF Single-Moment 6-class WSM6 schemes with CU Betts–Miller–Janjic (BMJ) has the ability to accurately predict and simulate extreme events in the region. According to [34], three heavy rainfall events across the southern peninsula of Malaysia were simulated using four distinct WRF CU schemes, including the new Kain–Fritsch, Betts–Miller–Janjic, Grell–Devenyi ensemble scheme, and the older Kain–Fritsch scheme. Despite generally better performance, Betts–Miller–Janjic created uncertainty while simulating the first rainfall event, suggesting that CU suitability may depend on the circumstances. It is crucial to investigate the effects of multiple parameterizations in an ensemble mode because the performance of one scheme is likely to be influenced by the other model configurations investigated. For instance, the findings on which CU scheme performs best would be intimately connected to the MP or land surface options considered during the model simulations [35].

With the above-mentioned perspectives, this study aimed to determine the best suitable physics scheme combination that can efficiently forecast the rainfall events at the KRB. KRB has been experiencing floods for decades due to its tropical climatic condition, which promotes torrential rainfall occurrences. The worst recorded KRB floods occurred in January1970, December 2001 and 2010, January 2011 and 2012, and December 2013, 2014, and 2021 [36,37]. All the flood events were caused by unpredicted heavy rain during the North East Monsoon (NEM), and the massive floods have imposed a severe risk to the local society. For this reason, significant hydro-meteorological forecasting is essentially important for decision-makers and scientific society to produce an effective hazard response that can reduce the risk of economic loss, property damages, and loss of human lives. Based on previous studies, the intensive prolonged rainfall during the monsoon period has caused flooding which resulted in severe damages to agricultural networks, infrastructure, properties, and loss of lives, predominantly in low lying areas of the east coast region [36,38–40]. To achieve this goal, the study focuses on statistical evaluation by conducting sensitivity analysis of different WRF physical schemes combinations to predict the moderate, heavy, and extreme rainfall events. This research utilized $1^\circ \times 1^\circ$ re-analysis data from the National Centre for Environmental Prediction (NCEP) Global Final Analysis (FNL) as the boundary conditions for the model simulations.

2. Materials and Methods

2.1. Study Area

The Kuantan River Basin (KRB) is the most important river basin in the northeastern end of the Pahang state in Peninsula Malaysia, where the only city, Kuantan City, is located. The basin lies between the coordinates of latitude 3.65° N to 4.13° N and longitude 102.86° E to 103.37° E, having a catchment area of 1630 km^2 where the Kuantan River begins from Sg. Lembing, passing through Kuantan City and ending at the South China Sea. The KRB consists of various land uses such as rural, agricultural, urban, and industrial areas. Based on the location, KRB has a tropical climatic condition with mean annual rainfall of approximately 2500 mm which, according to the historical record, often experiencing concurrent severe floods during the monsoon season. During the NEM season from October to March, prolonged heavy rainfall has caused river overflow, which consequently inundates low-lying areas and hampers human social life and the economy. In recent years, the worst flood events in KRB have brought huge destruction to agricultural activities and properties and caused loss of lives. Reportedly, around 14,044 to 18,000 people were affected and about 2294 km^2 of land was damaged [41,42]. Rapid urban development has reduced the capacity of river catchments that can be used to store and retain excess runoff, which results in frequent flood occurrences in the urbanized areas.

2.2. Location of Hydrological Stations

Several site visits have been made throughout the study. The main purpose of the visits was to rectify the actual locations of the hydrological stations. A Global Positioning System (GPS) device, the Garmin GPSMAP 76CSx model, was used to collect and record the coordinates of all the hydrological gauging stations. The updated locations are provided in Table 1. The total of eight rainfall stations were located within the KRB and one rainfall station (Pulau Manis) was slightly outside the boundary. In this basin, it was found that there is only one streamflow station situated at the upstream of the basin at Bukit Kenau. The KRB boundary and the selected rainfall hydrological stations identified for this study are presented in Figure 1.

Table 1. Location of the hydrological gauging stations in KRB.

No	Gauge Type	Station ID	Station Name	Latitude	Longitude
1	Rainfall	3732021	Kg. Sg. Soi	3.72°	103.29°
2	Rainfall	3631001	Pulau Manis	3.65°	103.11°
3	Rainfall	3732020	Paya Besar	3.77°	103.28°
4	Rainfall	3930012	PCCL Sg.Lembing	3.91°	103.03°
5	Rainfall	3832015	Rumah Pam	3.85°	103.25°
6	Rainfall	3731018	JKR.Gambang	3.71°	103.13°
7	Rainfall	3931013	Ladang Nada	3.90°	103.10°
8	Rainfall	3931014	Ladang Kuala Raman	3.89°	103.14°
9	Rainfall	3833001	JPS Negeri Pahang	3.82°	103.28°
10	Streamflow	3930401	Bukit Kenau	3.93°	103.06°

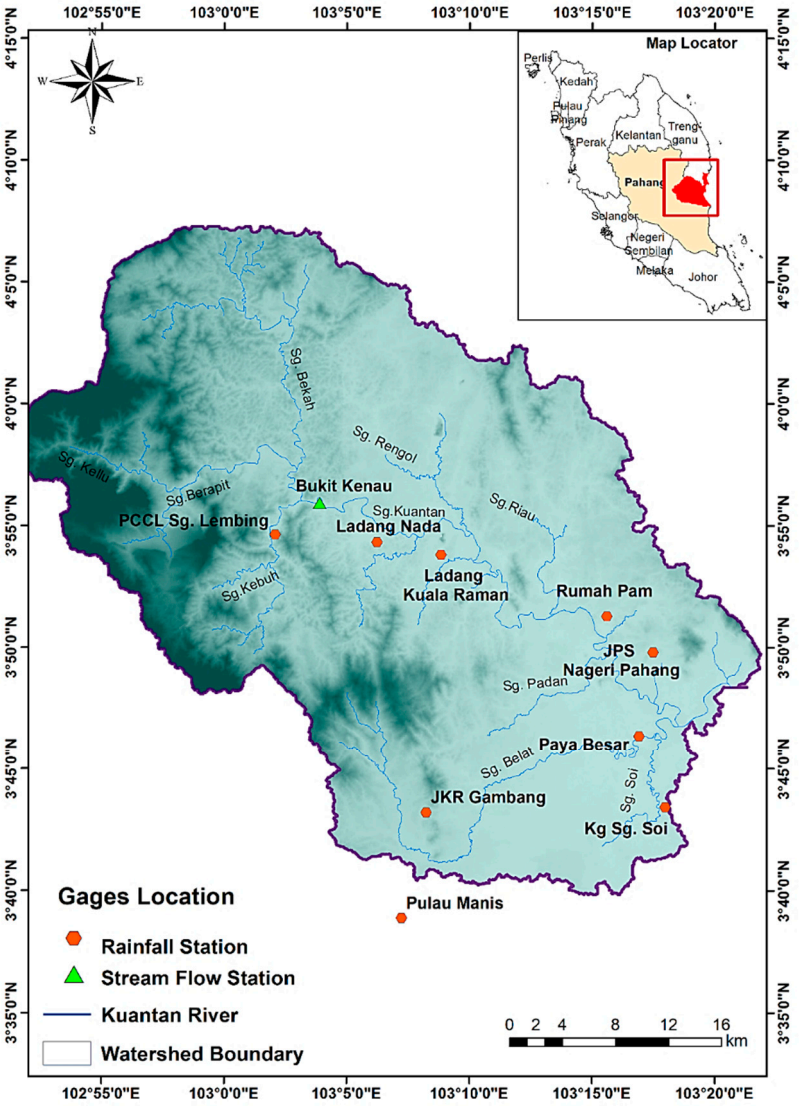

Figure 1. Study area of Kuantan River Basin and its hydrological gauging stations.

2.3. Collection of Data

This study utilized a 30 m resolution of the Shuttle Radar Topography Mission (SRTM)–Digital Elevation Model (DEM) to delineate the watershed boundary. The 30 m resolution was selected because it is the highest resolution that is freely available and can be downloaded from the United States Geological Survey (USGS) database. In this research, the time series rainfall and streamflow data from nine rainfall stations were collected from Drainage and Irrigation Department (DID). The acquired rainfall data were used in the WRF model schemes analysis. Table 2 provides general information on all the data collected for this study.

Table 2. General information on the primary data collected.

Data Required	Format	Source	Reference
Digital Elevation Model (DEM) from SRTM	30 (m) raster/Geotiff	Online Public domain source provided by NASA	www.srtm.csi.cgiar.org (accessed on 24 March 2017)
Rainfall gauge data	Vector format/Attribute data	DID, Pahang/Field survey	www.water.gov.my (accessed on 19 September 2017)

2.4. Categorization of Rainfall Event

The events were selected based on the periods when most of KRB experienced flooding. The time intervals of the hydrological data were 15 and 60 min for rainfall and 15 min for streamflow. Since the focus of the study is to stimulate event-based rainfall, the years 2001, 2010, 2011, 2012, 2013, and 2016 were selected because these years are predominant years for receiving rainfall and have provided more rainfall and streamflow data compared to other years [38,43]. For the study, rainfall periods that met the requirement of receiving both heavy rainfall and high streamflow were selected (see Appendix A). For the WRF model analysis and validation processes, the selected rainfall events were grouped into three categories: extreme, heavy, and moderate events. This categorization was implemented to evaluate the capability of the WRF model in estimating precipitation outputs that potentially contribute to flood events. The amount of rainfall in the watershed at the time of the event was used to categorise the events as extreme, heavy, and moderate. Three to five days of average total rainfall that exceeds three hundred fifty millimeters is considered an extreme event. Similar to this, heavy and moderate events are classified when the average total rainfall amounts over the same duration fall between 150 and 350 mm and less than 150 mm, respectively. Table 3 below shows the category of rainfall events based on the rainfall depth range.

Table 3. Categorization of rainfall events.

Rainfall Event	Event End Date	Total Rainfall Depth (mm)	Event Category
21 December 2001	23 December 2001	376.1	Extreme
29 December 2010	2 January 2011	281.0	Heavy
26 January 2011	30 January 2011	190.8	Heavy
26 March 2011	30 March 2011	58.5	Moderate
11 January 2012	13 January 2012	283.7	Heavy
1 December 2013	5 December 2013	764.3	Extreme
8 December 2016	12 December 2016	49.7	Moderate

There were 48 different combinations of model schemes tested using a single rainfall event to identify the most appropriate schemes combination among all applied combinations. Subsequently, the selected parameterized schemes were used to simulate other selected rainfall events. Figure 2 shows the methodological workflow for the present research.

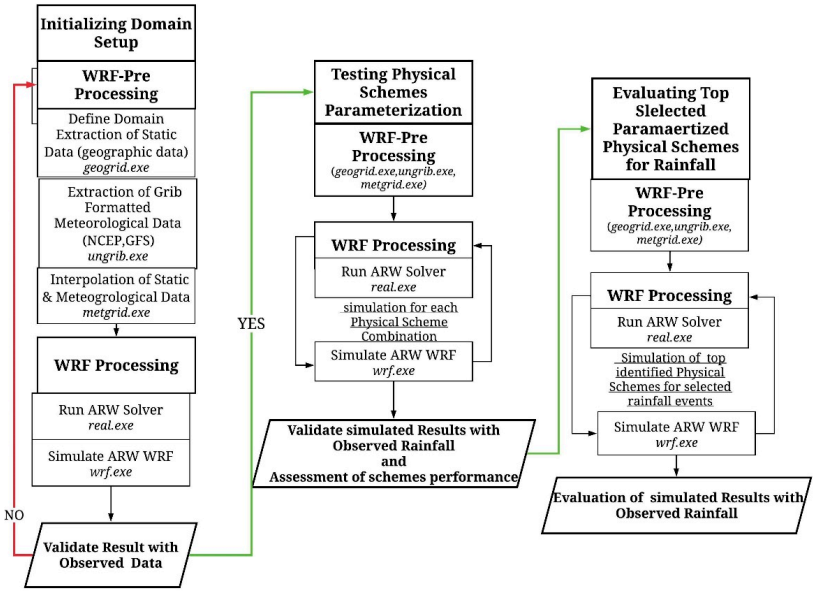

Figure 2. Methodological workflow.

2.5. Configuration of WRF Model Domain

In this study, the WRF model version 3.9.1 manufactured by National Center for Atmospheric Research (NCAR), Boulder, United State of America (USA), was used to estimate the rainfall in KRB. The methodology of designing the WRF model involves domain selection, resolution, projection system, WRF pre-processing, and WRF process. The selection of the domain is essentially required to design the experiments, especially for a mesoscale model. A new generation of the mesoscale model has higher resolutions compared to the global model. High resolution often requires high computational cost; however, it can provide precise information about an area such as topography, albedo, temperature, air pressure, moisture, etc. Thus, the high-resolution domain was used in this study to avoid any potential missing data. Three interactive nesting domains were used in this study, as shown in Figure 3. The parent domain (d01) was set at a grid resolution of 36 km, and two child domains covered the grid spacing at 12 km (d02) and 4 km (d03) resolution. A nesting ratio of 3:1 was applied to maintain the model's stability. The selected domains covered Peninsular Malaysia (36 km) with 27 grid points in the west–east (e_we) and 33 grid points in the south–north (e_sn) direction. The other two domains (12 km and 4 km) covered the east coast part of Peninsular Malaysia with grid points 31, 34, and 55, with 64 respective to the west–east (e_we) and south–north (e_sn) directions. This study used the high-resolution 4 km domain output of the rainfall series.

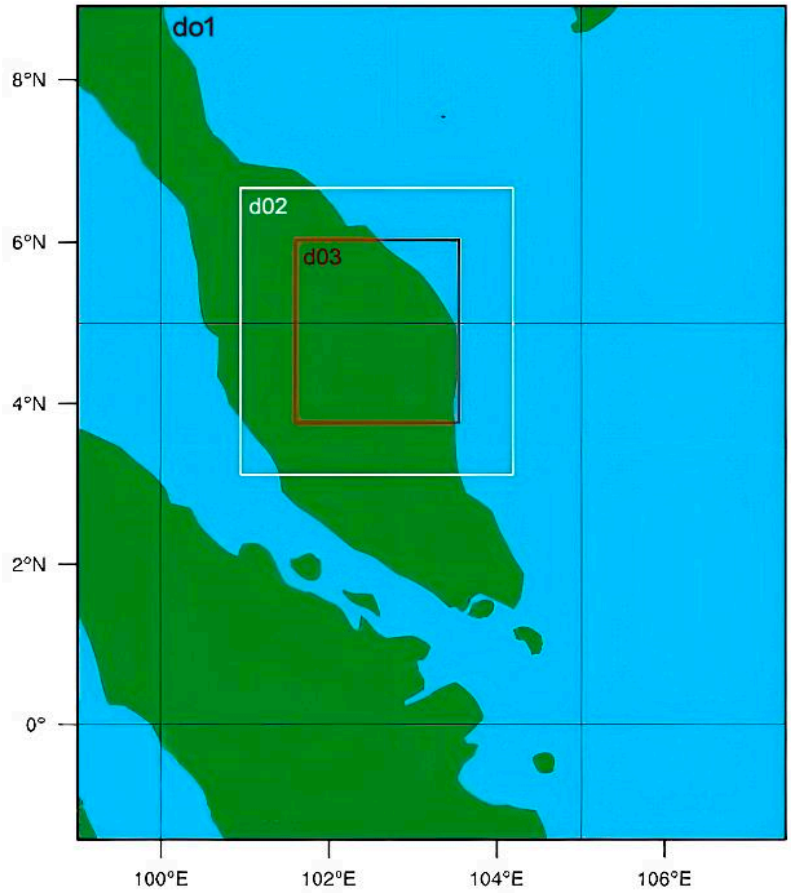

Figure 3. WRF domain configuration (36 km, 12 km, and 4 km resolutions).

2.6. Selection of Schemes for Model Sensitivity Test

In this research, the combinations of different physical schemes' parameterization were tested in the WRF model to determine the best combination. The sensitivity of each combination was evaluated by comparing the estimated and observed rainfall following statistical indices. The WRF model offers numerous physics schemes options in which

MP and CU schemes are the options that are mainly responsible for estimating rainfall. Therefore, this study adopted only MP and CU schemes. Currently, there are 13 microphysics and 14 cumulus schemes available for model simulation [44]. It is to be noted that not every scheme is suitable for all regions and climatic conditions. The selection of the MP and CU physical schemes was made according to their characteristics, suitability, and reference to previous studies. The configured WRF model with the selected physical schemes combination was applied to simulate the selected rainfall events. For this study, the rainfall event from 29 December 2010 to 2 January 2011 was used for evaluation of the performance of the physical scheme. Tables 4–6 describe the configuration of the selected physical schemes and designed domain used in estimating rainfall for the selected events.

Table 4. Combination of WRF physical schemes with selected MP and CU.

Physics Options	WRF Model Configured Scheme
Long Wave Radiation	RRTM Rapid radiative transfer model
Short Wave Radiation	Dhudiha Scheme MM5 short wave
Surface layer	Monin–Obukhov similarity theory
Planetary Boundary Layer	Yousei University (YSU) PBL scheme

Table 5. Combination of different microphysics and cumulus schemes.

S. No.	Microphysics Scheme	Cumulus Schemes	Schemes Name	Simulation Codes
1	Kessler	Kain–Fritsch	KSKF	MP1CU1
2	Kessler	Betts–Miller–Janjic	KSBMJ	MP1CU2
3	Kessler	Grell–Freitas	KSGF	MP1CU3
4	Kessler	Grell 3D	KSG3D	MP1CU5
5	Kessler	Tiedke	KSTiS	MP1CU6
6	Kessler	Old Kain–Fritsh	KSOKF	MP1CU99
7	Lin et al.	Kain–Fritsch	LinKF	MP2CU1
8	Lin et al.	Betts–Miller–Janjic	LinBMJ	MP2CU2
9	Lin et al.	Grell–Freitas	LinGF	MP2CU3
10	Lin et al.	Grell 3D	LinG3D	MP2CU5
11	Lin et al.	Tiedke	LinTiS	MP2CU6
12	Lin et al.	Old Kain–Fritsh	LinOKF	MP2CU99
13	WRF Single Moment 3 class	Kain–Fritsch	WSM3KF	MP3CU1
14	WRF Single Moment 3 class	Betts–Miller–Janjic	WSM3BMJ	MP3CU2
15	WRF Single Moment 3 class	Grell–Freitas	WSM3GF	MP3CU3
16	WRF Single Moment 3 class	Grell 3D	WSM3G3D	MP3CU5
17	WRF Single Moment 3 class	Tiedke	WSM3TiS	MP3CU6
18	WRF Single Moment 3 class	Old Kain–Fritsh	WSM3OKF	MP3CU99
19	WRF Single Moment 6 class	Kain–Fritsch	WSM6KF	MP6CU1
20	WRF Single Moment 6 class	Betts–Miller–Janjic	WSM6BMJ	MP6CU2
21	WRF Single Moment 6 class	Grell–Freitas	WSM6GF	MP6CU3
22	WRF Single Moment 6 class	Grell 3D	WSM6G3D	MP6CU5
23	WRF Single Moment 6 class	Tiedke	WSM6TiS	MP6CU6
24	WRF Single Moment 6 class	Old Kain–Fritsh	WSM6OKF	MP6CU99
25	Goddard Microphysics	Kain–Fritsch	GoMKF	MP7CU1
26	Goddard Microphysics	Betts–Miller–Janjic	GoMMBJ	MP7CU2
27	Goddard Microphysics	Grell–Freitas	GoMGF	MP7CU3
28	Goddard Microphysics	Grell 3D	GoMG3D	MP7CU5
29	Goddard Microphysics	Tiedke	GoMTiS	MP7CU6
30	Goddard Microphysics	Old Kain–Fritsh	GoMOKF	MP7CU99
31	New Thompson et al.	Kain–Fritsch	NThKF	MP8CU1
32	New Thompson et al.	Betts–Miller–Janjic	NThBMJ	MP8CU2
33	New Thompson et al.	Grell–Freitas	NThGF	MP8CU3
34	New Thompson et al.	Grell 3D	NThG3D	MP8CU5
35	New Thompson et al.	Tiedke	NThTis	MP8CU6
36	New Thompson et al.	Old Kain–Fritsh	NThOKF	MP8CU99

Table 5. *Cont.*

S. No.	Microphysics Scheme	Cumulus Schemes	Schemes Name	Simulation Codes
37	Morrison Double Moment	Kain–Fritsch	MDMKF	MP10CU1
38	Morrison Double Moment	Betts–Miller–Janjic	MDMBMJ	MP10CU2
39	Morrison Double Moment	Grell–Freitas	MDMGF	MP10CU3
40	Morrison Double Moment	Grell 3D	MDMG3D	MP10CU5
41	Morrison Double Moment	Tiedke	MDMTiS	MP10CU6
42	Morrison Double Moment	Old Kain–Fritsh	MDMOKF	MP10CU99
43	Stony Brook University (Y Lin)	Kain–Fritsch	SBUKF	MP13CU1
44	Stony Brook University (Y Lin)	Betts–Miller–Janjic	SBUBMJ	MP13CU2
45	Stony Brook University (Y Lin)	Grell–Freitas	SBUGF	MP13CU3
46	Stony Brook University (Y Lin)	Grell 3D	SBUG3D	MP13CU5
47	Stony Brook University (Y Lin)	Tiedke	SBUTiS	MP13CU6
48	Stony Brook University (Y Lin)	Old Kain–Fritsh	SBUOKF	MP13CU99

Table 6. Configured domain for the study.

Description	Detail
Maximum Domain	3
Domain Extent	100° East to 108° East, 0° North to 8° North
Domain Spatial Resolution	36 km (D1), 12 km (D2), 4 km (D3)
Static Geographic data Resolution	10 m, 2 m and 3 s
Grid Ratio	1:3
Grid Size	27 × 33 (D1), 31 × 34 (D2) and 55 × 64 (D3)
Map Projection	Mercator
Reference Latitude	3.76
Reference Longitude	103.22
True Median Latitude	3.76
Standard Longitude	103.22

2.7. Evaluation Methods for Model Performance

Several statistical indices are widely used in the models' evaluation, which includes Root Mean Square Error (RMSE) and Percentage Error (PE) and the contingency table matrix. The relative statistical methods of the contingency table matrix are comprised of the Percentage of Correction, Hit Rate (HR), False Alarm Ration (FAR), Threat Score (TS), and Bias (B).

2.7.1. Root Mean Square Error

RMSE is the most commonly used method in model evaluation to measure the difference between the predicted (P) and observed (O) values [45]. The RMSE equation is as presented in Equation (1).

$$\mathrm{RMSE} = \sqrt{\frac{1}{n}\sum_{i=1}^{n}(P_i - O_i)} \quad (1)$$

where n is the number of sample points, P is the predicted value, and O is the observed value.

2.7.2. Percentage Error

The Percentage Error (PE) is the simple statistical method which is used to determine the precision of the measured values and actual values. A difference of ±20% between actual and estimated values is acceptable in model evaluation [46]. PE helps to understand how accurate the measured values are to the real value. The PE is expressed in a percentage and was calculated from the equation:

$$\mathrm{PE} = \frac{(\text{measured value} - \text{actual value})}{(\text{actual value})} \times 100 \quad (2)$$

2.7.3. Contingency Table Matrix and Relatives Measures

The contingency table matrix describes the frequency distribution of the related variables considered in this study. Table 7 shows the matrix of the interrelated variables and their interaction. There are four possible outcomes produced in this analysis, which are:

Table 7. Contingency table matrix.

		Observed		
		Yes	**No**	
Forecast	Yes	a	b	a + b
	No	c	d	c + d
		a + c	b + d	n = a + b + c + d

a = The event is forecasted and occurred.
b = The event is forecasted but not occurred.
c = The event is not forecasted but occurred.
d = The event is not forecasted and not occurred.

The related statistical methods were performed according to the interrelated variable presented in the contingency table matrix [47].

2.7.4. Percentage of Correction

Percentage of Correction is the most direct and spontaneous method to evaluate model accuracy. PC defines the percentage of the number of forecasts that are correct. The value of PC ranges from 0 to 1 with the indicator of no correct forecast observed to all correct forecast observed [48]. This statistical method is significant in high-frequency forecasting. PC is calculated as:

$$PC = \frac{(a + d)}{n} \quad (3)$$

2.7.5. Hit Rate

HR is commonly known as the Probability of Detection (POD). This measure was used to determine the fraction of the observed events' forecasting correctly. It is calculated as:

$$HR = \frac{a}{(a + c)} \quad (4)$$

The HR values range from (0), which indicates a poor fraction to (1) that shows good fraction or correct forecast [47].

2.7.6. False Alarm Ratio

False Alarm Ratio (FAR) is the fraction of "true or yes" forecasted events that were wrongly predicted. The best possibility of the model is presented by zero (0) value and the poor possibility indicated by the value 1. FAR was calculated using Equation (5).

$$FAR = \frac{b}{(a + b)} \quad (5)$$

2.7.7. Threat Score

Threat Score (TS) is another alternate intuitive indicator to calculate the event forecasting accuracy. This method is also known as the Critical Success Index (CSI). TS is the number of correct forecasts divided by the total number of observed forecasts that occurred. This can be regarded as the proportion of correct forecasts [48]. It is expressed as follows:

$$TS = \frac{a}{a + b + c} \quad (6)$$

The TS score ranges from (0), which is the worst possible forecast to (1), which is at the best end.

2.7.8. Bias

Bias (B) is often used to represent the verification ratio of the contingency table matrix. B is the comparison between the number of times the event was forecasted and occurred [49]. It was calculated using Equation (7).

$$B = \frac{a + b}{a + c} \quad (7)$$

B < 1 means the event forecasted less than the event occurred (underestimate).
B = 1 means the event forecasted the same as the event occurred (unbiased).
B > 1 means the event forecast more the event occurred (overestimate).

3. Results

The performances of physical schemes' parameterization in the WRF model have been estimated through testing of the selected 48 different combinations. Different statistical methods were applied to evaluate the performance of the model schemes. This section presents the results from several statistical techniques in analyzing the accuracy and performance of each combination of WRF physical schemes to produce reliable rainfall estimation in KRB.

3.1. Model Schemes Evaluation

The sensitivities of the 48 physical scheme combinations in the WRF model have been evaluated using a variety of statistical approaches. Based on the statistical analysis, the physical scheme combinations have been ranked to determine the most efficient physical scheme combinations for KRB. The ranking of the WRF scheme's performance was in accordance to the rainfall event selected from 29 December 2010 to 2 January 2011. The cumulative ranks were applied to determine the total ranking for each scheme combination. Different schemes performed differently depending on the computed Root Mean Square Error (RMSE) at each rainfall station as shown in Table A1 in Appendix A. From the statistical result, it was found that the Stony Brook University Grell Freitas (SBUGF) schemes performed exceptionally well at downstream region of KRB, consisting of the stations Kg. Sg. Soi., Pulau Manis, and the Malaysian Public Works Department (JKR) Gambang. Scheme LinGF, on the other hand, did well at the stations Ladang Nada and Ladang Kuala Raman. The SBUKF and SBUBMJ schemes were found effective at stations JPS Negeri Pahang, Paya Besar, and Rumah Pam.

According to the computed PC in Figure 4, the majority of the model simulations indicated insufficient event occurrence at stations JPS Negeri Pahang, Rumah Pam, PCCL Sg. Lembing, Paya Besar, Ladang Nada, and Ladang Kuala Raman. However, distinct model scheme combinations, which include SBUOKF, GoMKF, SBUBMJ, MDMBMJ, NthBMJ, and SBUGF, have been identified as capable of capturing the event at all stations with PC ranges from 0.52 to 0.79. It is noteworthy that the same model schemes, except for SBUGF, were able to reliably anticipate rainfall based on the determined Threat Score (TS) ranges from 0.5 to 0.79 (see Figure 5), particularly for stations downstream of the KRB, while WSM3OKF schemes have a low TS among all. The most well-known method of calculating the percentage of hit rate was also used to determine the correctness of model schemes. The value hit to a score of 1 is defined as the best-fit forecasting. All the model parameterized schemes performed adequately for stations Kg. Sg. Soi, Pulau Manis, and JKR Gambang, as shown in Figure 6, whereas combinations of schemes SBUKF, GoMKF, MDMBMJ, SBUGF, and SBUBMJ performed exceptionally well in predicting rainfall events for all of the stations' ranges from 0.6 to 1.

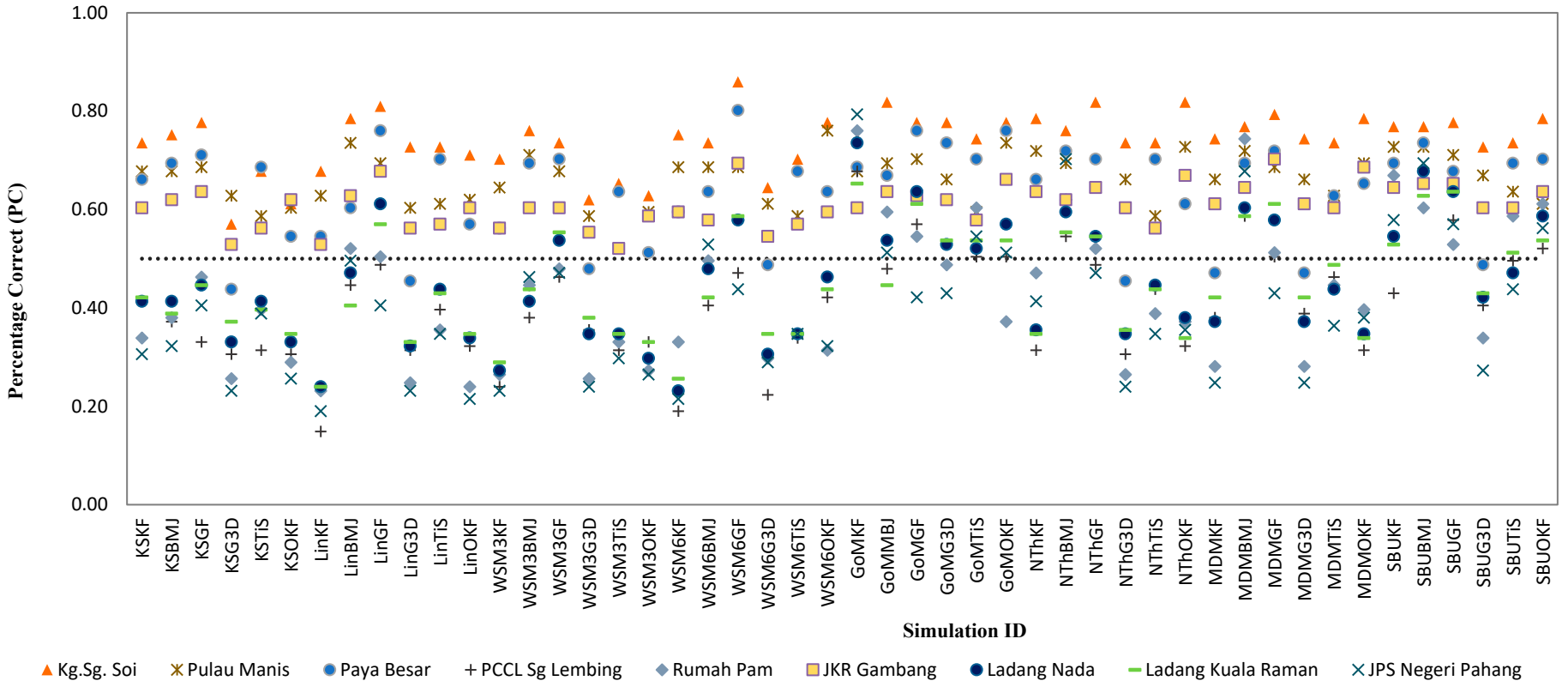

Figure 4. Percentage correct for the WRF physical schemes combination at each station of KRB.

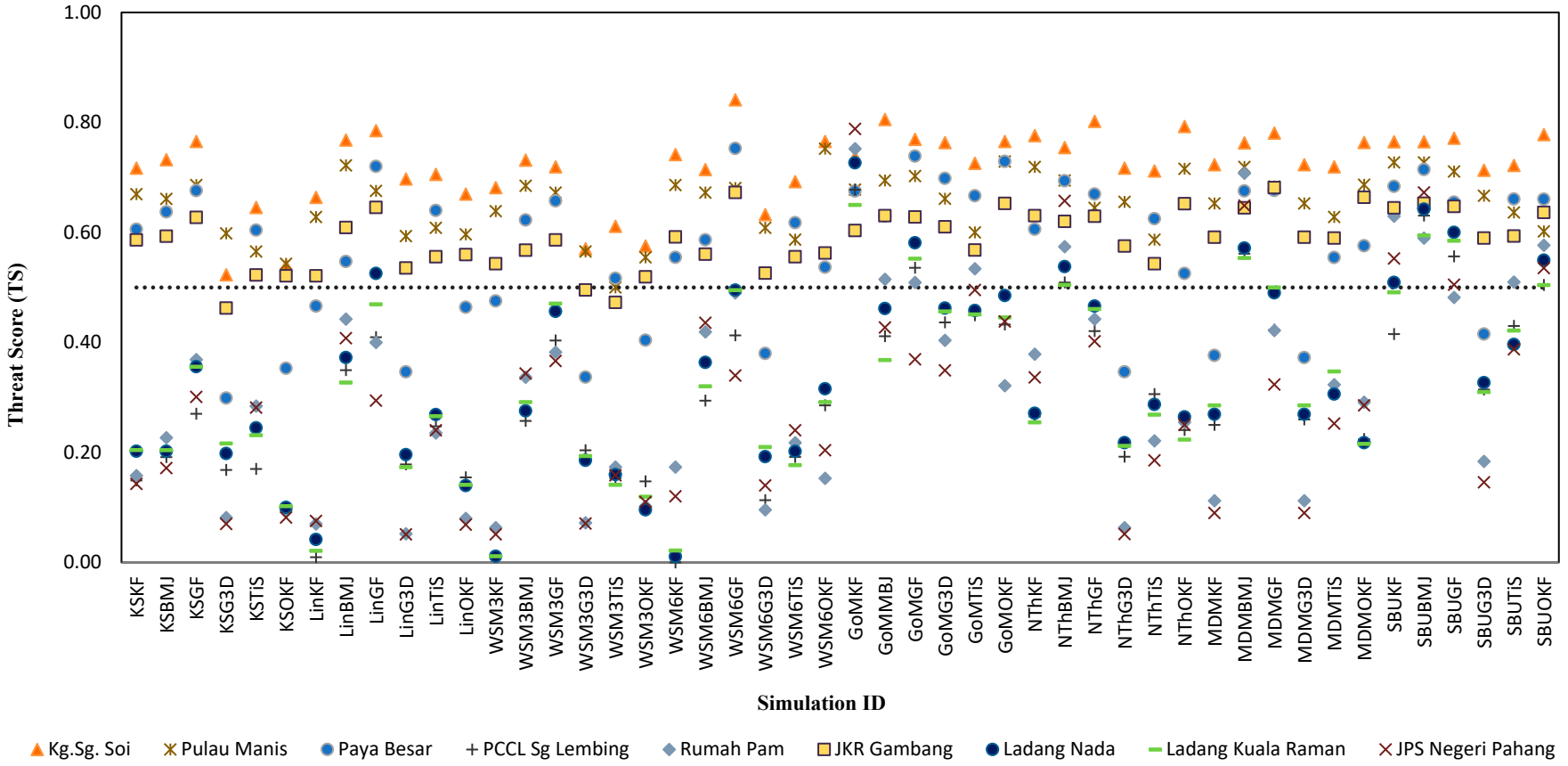

Figure 5. Threat Score (TS) for the WRF physical schemes combination at each station of KRB.

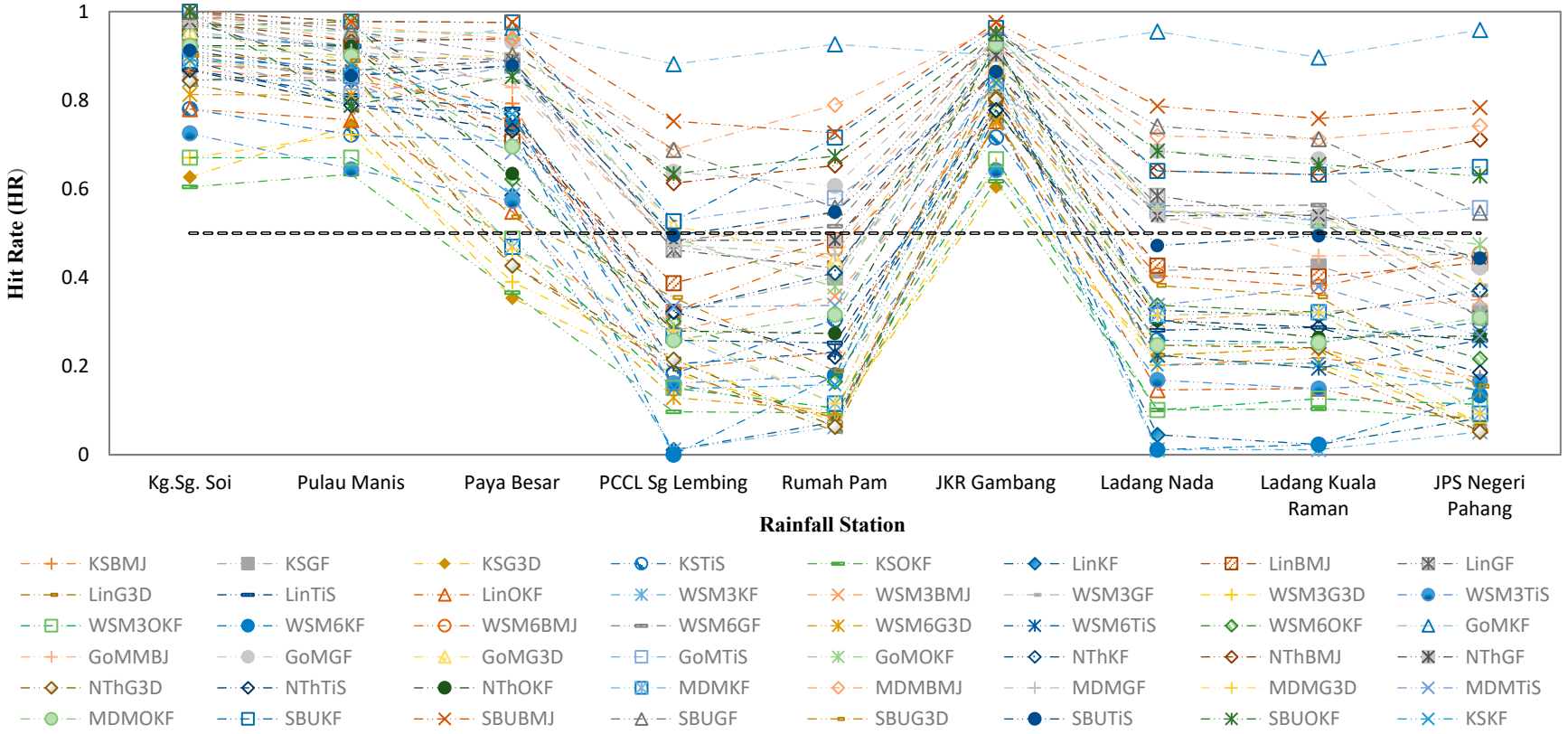

Figure 6. Hit Rate (HR) for the WRF physical schemes combination at each station of KRB.

Furthermore, the False Alarm Ratio (FAR), which is another more widely used statistical method in weather forecasting, indicates that the majority of the model simulation shows great efficiency at the upper stream part of KRB, where the stations PCCL Sg. Lembing, Rumah Pam, Ladang Nada, and Ladang Kuala Raman are located. According to the FAR method, a low number of false alerts means higher accuracy. Figure 7 shows the WSM3KF (0.00) and KSKF (0.00–0.05) schemes have the maximum efficiency. Model accuracy assessment was further investigated using Bias (B). A statistical estimator was used to calculate the ratio of an event's forecast to the total observed values. With an unbiased forecast, a forecasted value of 1 reflects the best performance. The results in Figure 8 revealed that all schemes' simulations produced predicted events (>1) at the downstream part and underpredicted (<1) at the upstream of KRB, though the combination of SBUBMJ schemes produced a relatively better output among all.

Overall, the accuracy of the 48 distinct scheme combinations was measured using TS, HR, PC, RMSE, FAR, and Bias. The scheme simulations were shown to be highly efficient using TS, while the percentage of false alarms was detected using FAR. The schemes were ranked according to their obtained values on each of the indices (described in Section 2.6). All of the evaluated ranks were combined to find the set of top performance scheme combinations. Table A2 shows the overall ranking of the model schemes that have been investigated. There are five highly efficient scheme combinations which have been identified. These schemes were then used to simulate rainfall events of various types (extreme, heavy, and moderate) to ensure their accuracy and find the best scheme combination for KRB. Schemes SBUBMJ were ranked first in the cumulative ranking for their significant performance in estimating rainfall for the event. WSM6GF, LinGF, MDMBMJ, and MDMGF were ranked second to fifth, respectively. Table 8 shows the top five WRF physical scheme combinations in terms of performance.

Table 8. Selected top performance of WRF physical schemes combination.

Simulation Code	Simulation Names	Microphysics Schemes (MP)	Cumulus Schemes (CU)	Schemes Rank
MP13CU2	SBUBMJ	Stony Brook University	Betts–Miller–Janjic	1
MP6CU3	WSM6GF	WRF Single Moment 6 class	Grell–Freitas	2
MP2CU3	LinGF	Lin et al.	Grell–Freitas	3
MP10CU2	MDMBMJ	Morrison Double Moment	Betts–Miller–Janjic	4
MP10CU3	MDMGF	Morrison Double Moment	Grell–Freitas	5

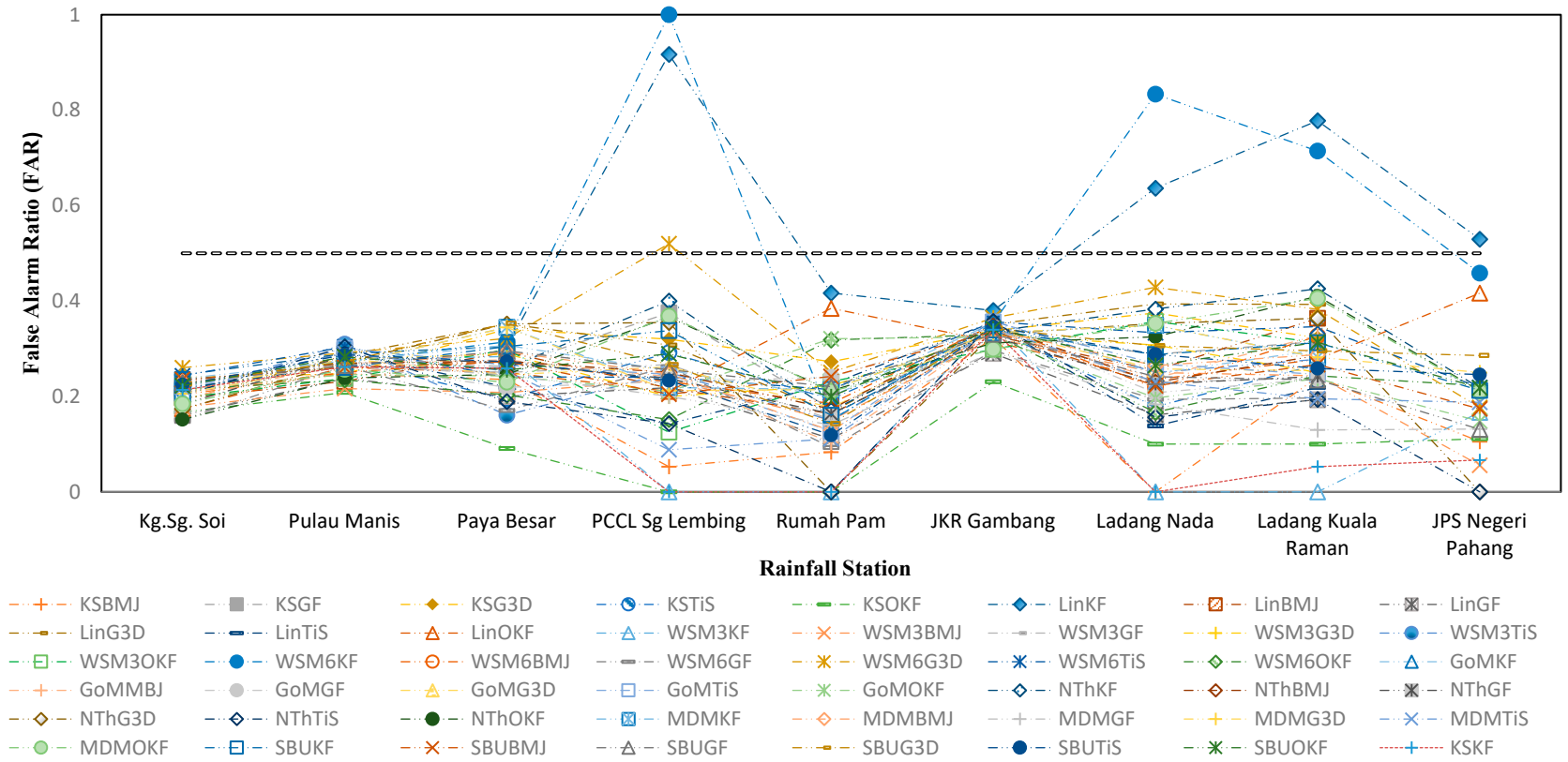

Figure 7. False Alarm Ratio (FAR) for the WRF physical schemes combination at stations of KRB.

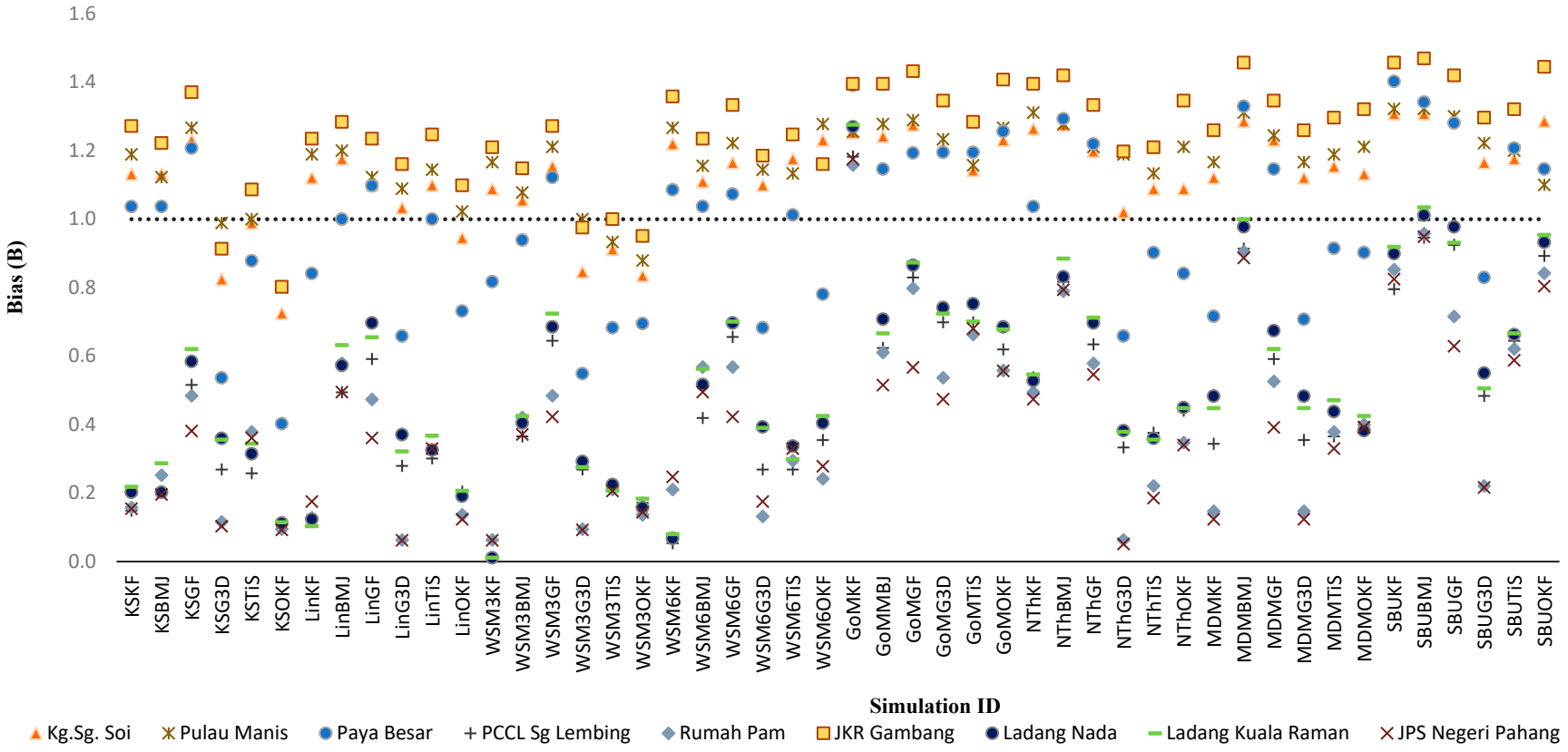

Figure 8. Bias (B) for the WRF physical schemes combination at each station of KRB.

3.2. Performance of the Schemes Combination in Predicting Rainfall

The top five physical scheme combinations obtained have been applied to estimate the extreme, heavy, and moderate rainfalls. Two precipitation events from 21 to 23 December 2001 and 1 to 3 December were selected for the extreme rainfall evaluations. The result for the event from 21 to 23 December 2001, displayed in Figure 9, indicated that the schemes WSM6GF, MDMGF, and LinGF seem to produce low rainfall magnitude at all stations compared to the observed. Meanwhile, the schemes SBUBMJ and MDMBMJ produced overestimated rainfall at stations Kg. Sg Soi (30% and 5%), Rumah Pam (58% and 6%), Ladang Nada (25% and 16%), Ladang Kuala Raman (79% and 66%), and JPS Negeri Pahang (96% and 73%), respectively. The good agreement of both SBUBMJ and MDMBMJ was noticed at station PCCL Sg Lembing. Overall, MDMBMJ performed relatively better in estimating rainfall with an average Percentage Error (PE) of about 31.8%, as shown in Table 9.

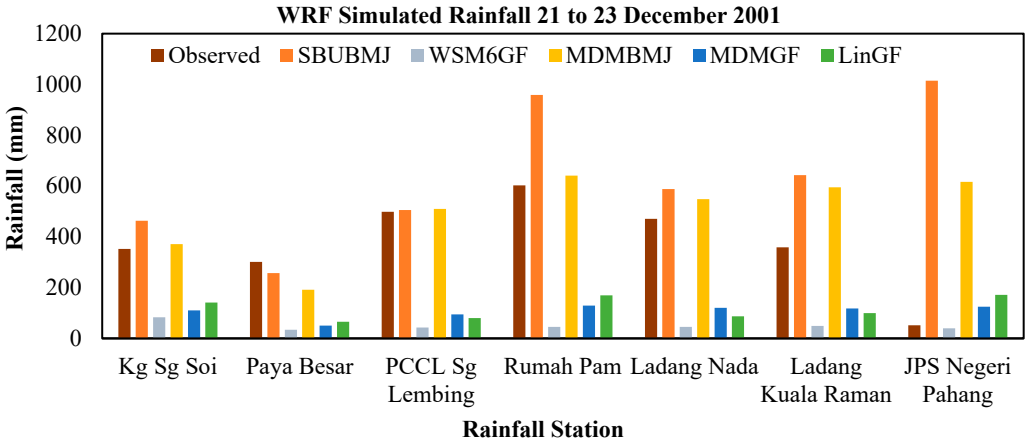

Figure 9. WRF simulated rainfall for the 21 to 23 December 2001 event.

Table 9. Comparison of the average total average rainfall depth estimated by WRF schemes and observed data for the 21 to 23 December 2001 event in KRB.

WRF Schemes	Ranked	Average Total Observed Rainfall Depth (mm)	Average Total WRF Rainfall Depth (mm)	PE (%)
SBUBMJ	1	376.1	632.51	68.2
WSM6GF	2		48.04	−87.2
LinGF	3		115.9	−69.2
MDMBMJ	4		495.9	31.8
MDMGF	5		106.4	−71.7

The performance of the schemes was further tested for the event on 1 to 3 December 2013, with the result present in Figure 10. The comparison has been limited to accessible rainfall stations due to a lack of observed data. According to the results, it is found that all of the schemes' combinations were unable to predict rainfall accurately at stations JKR Gambang, Rumah Pam, and Kg. Sg. Soi. However, when compared to the observed rainfall at station Ladang Nada, the LinGF schemes overestimated rainfall by about 49% whilst the scheme MDMGF showed better accuracy. Considering the estimated total average rainfall depth (see Table 10), all of the schemes showed underestimated rainfall with error differences ranging from 26.9% to 60% compared to observed data.

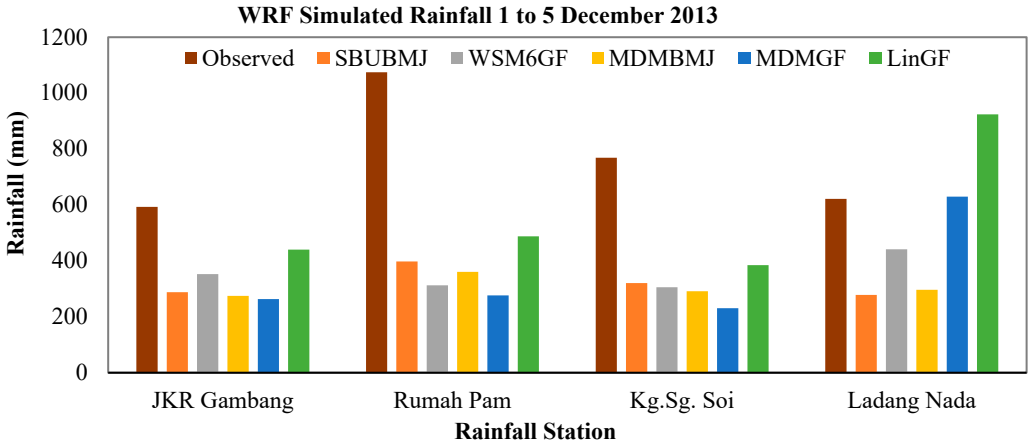

Figure 10. WRF simulated rainfall for the 1 to 5 December 2013 event.

Table 10. Comparison of average total rainfall depth estimated by WRF schemes and observed data for the 1 to 5 December 2013 event in KRB.

WRF Schemes	Ranked	Average Total Observed Rainfall Depth (mm)	Average Total WRF Rainfall Depth (mm)	PE (%)
SBUBMJ	1	764.3	320.593	−58.1
WSM6GF	2		352.5	−53.9
LinGF	3		558.7	−26.9
MDMBMJ	4		305.3	−60.0
MDMGF	5		349.6	−54.3

Figure 11 shows the predicted results for the event from 29 December 2010 to 2 January 2011, and Table 11 listed the magnitude of total average rainfall estimated by the WRF schemes. Results revealed that most of the schemes' combinations produced under predicted rainfall magnitude at different rainfall stations range, approximately, from 5% to 88% compared to the observed. Schemes SBUBMJ, on the other hand, generated about 20% overestimation for the rainfall at stations JKR Gambang and Kuala Raman. According to the obtained result at the station Ladang Nada, it has been observed that, except for the scheme MDMBM, all the other four scheme combinations accurately capture the precipitation intensity. Overall, SBUBMJ was found to be an effective scheme to simulate the event with slightly underestimated rainfall depth with a difference of about 7.5%.

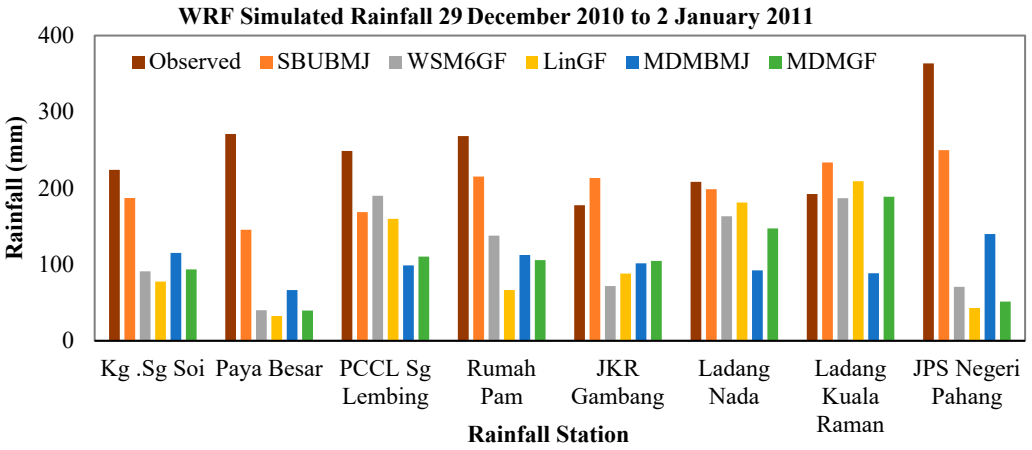

Figure 11. WRF Simulated rainfall for the 29 December 2010 to 2 January 2011 event.

Table 11. Comparison of average total rainfall depth estimated by WRF schemes and observed data for the 29 December 2010 to 2 January 2011 event in KRB.

WRF Schemes	Ranked	Average Total Observed Rainfall Depth (mm)	Average Total WRF Rainfall Depth (mm)	PE (%)
SBUBMJ	1	244.1	201.3	−17.5
WSM6GF	2		118.8	−51.3
LinGF	3		107.1	−56.1
MDMBMJ	4		101.7	−58.3
MDMGF	5		105.0	−57.0

Two other rainfall events first from 26 to 30 January 2011 and the second event from 11 to 13 January 2012 were selected to simulate heavy rainfall, as shown in Figures 12 and 13, respectively. The simulation's output for the first event is shown in Figure 12, where the results indicated that all the model schemes showed varied performance in terms of capturing the rainfall compared to the observed rainfall. It is worth noting that they were unable to capture the event intensity at station Paya Besar. Two model schemes combinations of MDMGF and LinGF produced over estimated rainfall at PCCL Sg Lembing and Ladang Nada and underestimated rainfall at station Rumah Pam and JPS Negeri Pahang. Overall, the schemes SBUBMJ produced greater accuracy, with a PE of about −21.2 percent, as shown in Table 12. Results obtained from simulation of the second event are displayed in Figure 13, where it is revealed that the five schemes produced lower rainfall (ranges from 20 mm to 200 mm) at various stations when compared to observed data. On the other hand, the cumulus scheme BMJ combined with MP schemes SBU and MDM provided approximately 7% to 20% overestimated rainfall at the station PCCL Sg. Lembing and JPS Negeri Pahang. Again, the combination of SBUBMJ schemes performed better in estimating the depth of average total rainfall in KRB, with the PE of about −21.8% overall, as shown in Table 13.

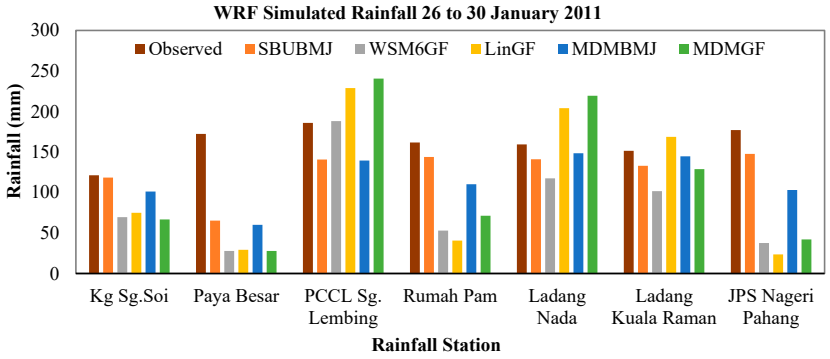

Figure 12. WRF simulated rainfall for the 26 to 30 January 2011 event.

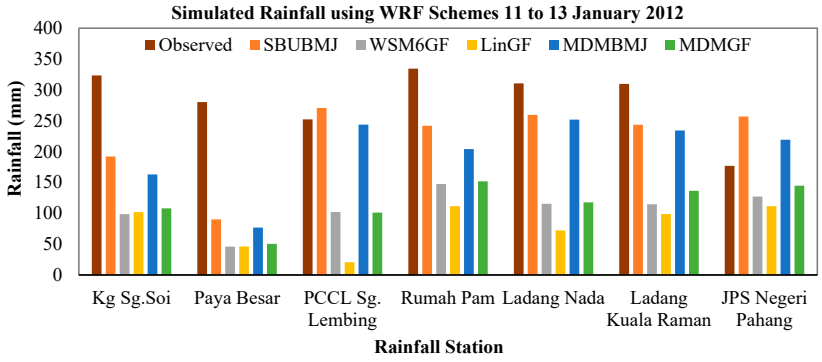

Figure 13. WRF simulated rainfall for 11 to 13 January 2012 event.

Table 12. Comparison of average total rainfall depth estimated by WRF schemes and observed data for the 26 to 30 January 2011 event in KRB.

WRF Schemes	Ranked	Average Total Observed Rainfall Depth (mm)	Average Total WRF Rainfall Depth (mm)	PE (%)
SBUBMJ	1	161.3	127.1	−21.2
WSM6GF	2		85.0	−47.3
LinGF	3		110.0	−31.8
MDMBMJ	4		115.3	−28.5
MDMGF	5		113.8	−29.4

Table 13. Comparison of average total rainfall depth estimated by WRF schemes and observed data for the 11 to 13 January 2012 event in KRB.

WRF Schemes	Ranked	Average Total Observed Rainfall Depth (mm)	Average Total WRF Rainfall Depth (mm)	PE (%)
SBUBMJ	1	283.8	221.88	−21.8
WSM6GF	2		107.1	−62.2
LinGF	3		80.2	−71.7
MDMBMJ	4		198.8	−29.9
MDMGF	5		115.6	−59.3

Figures 14 and 15 show the results of moderate rainfall model simulations for the events of 26 to 30 March 2011 and 8 to 12 December 2016, respectively. The acquired results from the event of 26 to 30 March 2011 revealed that the schemes WSM6GF, LinGF, and MDMGF estimated higher rainfall than the observed rainfall at all KRB stations. However, the parameterization of the BMJ cumulus scheme combines with microphysics in SBU, and MDM indicates good accuracy. MDMBMJ, on the other hand, overestimated rainfall at station JKR Gambang. As indicated in Table 14, the scheme SBUBMJ performed considerably better in simulating moderate rainfall in KRB, with a PE difference of about 22.2%. Furthermore, the simulation results for the event from 8 to 12 December 2016 revealed that the schemes WSM6GF, LinGF, and MDMGF generate overestimated rainfall at PCCL Sg. Lembeing, JKR Gambang, Ladang Nada, and Ladang Kuala Raman in comparison to observed rainfall, showing better accuracy at stations Kg. Sg. Soi and Rumah Pam. As indicated in Table 15, the model scheme MDMBMJ performed well among all, with a difference of −0.6% PE.

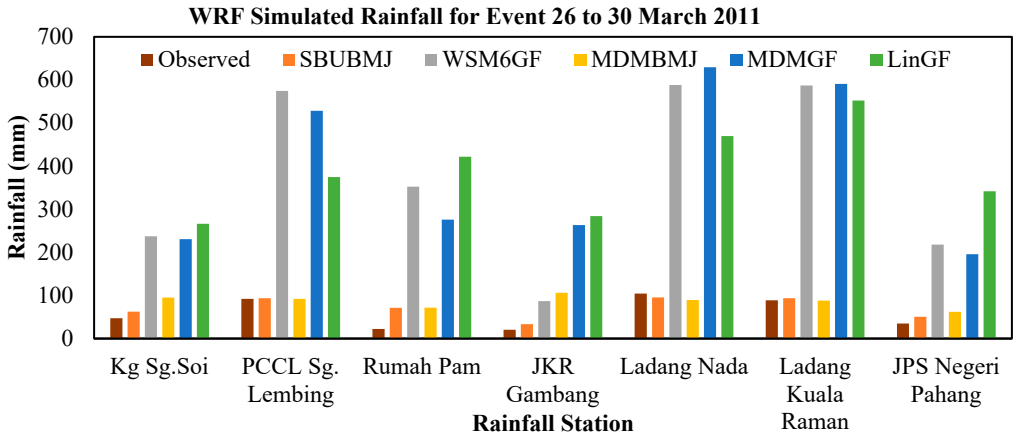

Figure 14. WRF simulated rainfall for 26 to 30 March 2011 event.

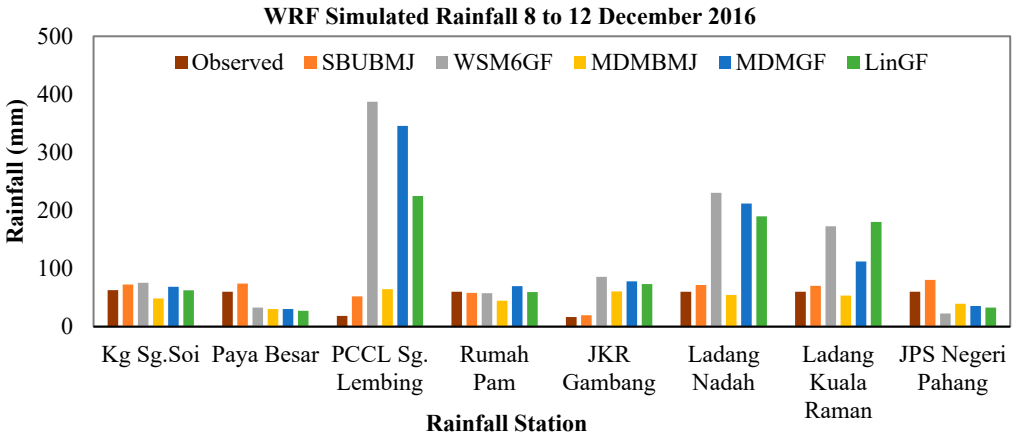

Figure 15. WRF simulated rainfall for 8 to 12 December 2016 event.

Table 14. Comparison of average total rainfall depth estimated by WRF schemes and observed data for 26 to 30 March 2011 event in KRB.

WRF Schemes	Ranked	Average Total Observed Rainfall Depth (mm)	Average Total WRF Rainfall Depth (mm)	PE (%)
SBUBMJ	1	58.4	71.295	22.2
WSM6GF	2		377.6	547.0
LinGF	3		386.9	563.0
MDMBMJ	4		86.1	47.5
MDMGF	5		387.5	564.0

Table 15. Comparison of average total rainfall depth estimated by WRF schemes and observed data for 8 to 12 December 2016 event in KRB.

WRF Schemes	Ranked	Average Total Observed Rainfall Depth (mm)	Average Total WRF Rainfall Depth (mm)	PE (%)
SBUBMJ	1	49.7	62.2	25.2
WSM6GF	2		133.0	167.4
LinGF	3		106.2	113.6
MDMBMJ	4		49.4	−0.6
MDMGF	5		118.9	139.1

3.3. The Spatial Rainfall Pattern Distribution

Figures 16–22 provide a comparison of observed and simulated WRF MPCU schemes for the selected rainfall event categories in terms of spatial interpolation of rainfall patterns using Inverse Distance Weighting (IDW). For the events on 21 to 23 December 2001 and 1 to 5 December 2013, the CU scheme BMJ parameterized with MP schemes MDM and SBU showed comparatively better performance than the other schemes' combinations in terms of capturing spatial patterns for extreme rainfall, respectively. The scheme cumulus GF, on the other hand, was found to be ineffective at producing spatial precision when combined with MP schemes Lin and MDM, respectively. Based on the results of simulating heavy rainfall events, it was found that all of the scheme combinations accurately captured the rainfall intensity at the upstream region of the KRB during the event from 26 to 30 January 2011. However, SBUBMJ showed a relatively better performance to capture the rainfall event overall. By comparing the results for the event on 29 December 2010 to 2 January 2011, it has been observed that the combination of MDMBMJ followed a similar rainfall distribution pattern as the observed pattern. It has also been noted that the schemes LinGF were unable to represent the correct rainfall pattern for the event on 11 to 13 January 2012, whereas the other scheme combinations performed well in the central region of KRB. In comparing the efficiency of the schemes in capturing the pattern of moderate rainfall events,

the results showed that the combination of schemes SBUMJ, WSM6GF, and MDMGF was capable of capturing the rainfall distribution pattern seen during the event from 26 to 30 March 2011. Moreover, SBUBMJ showed a tendency to accurately represent the event from 8 to 12 December 2011.

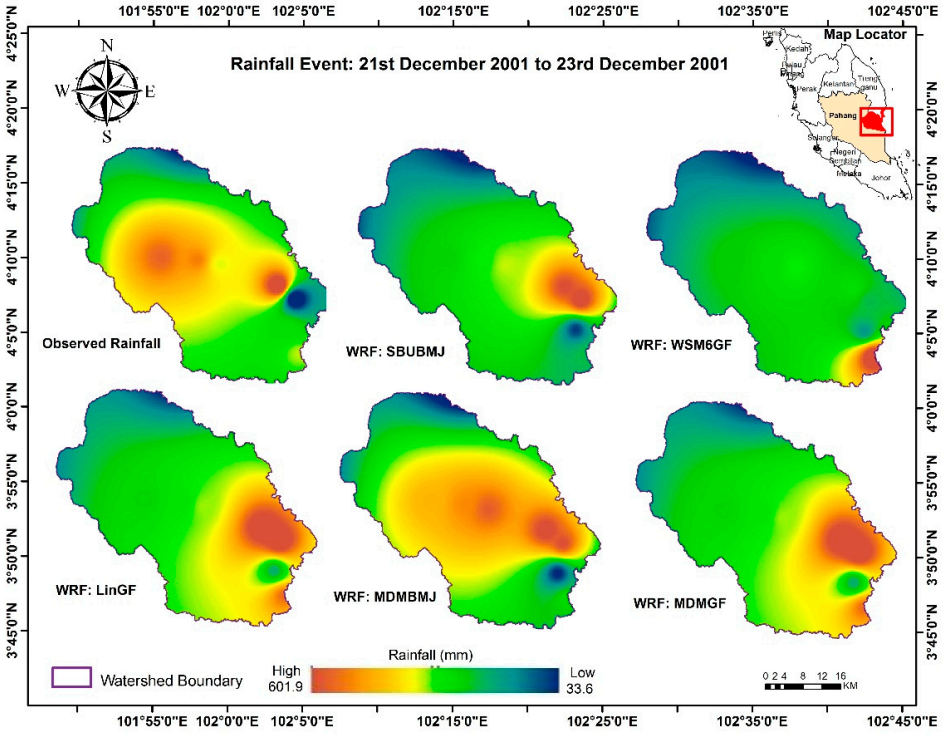

Figure 16. Spatial rainfall pattern for event from 21 to 23 December 2001 in KRB.

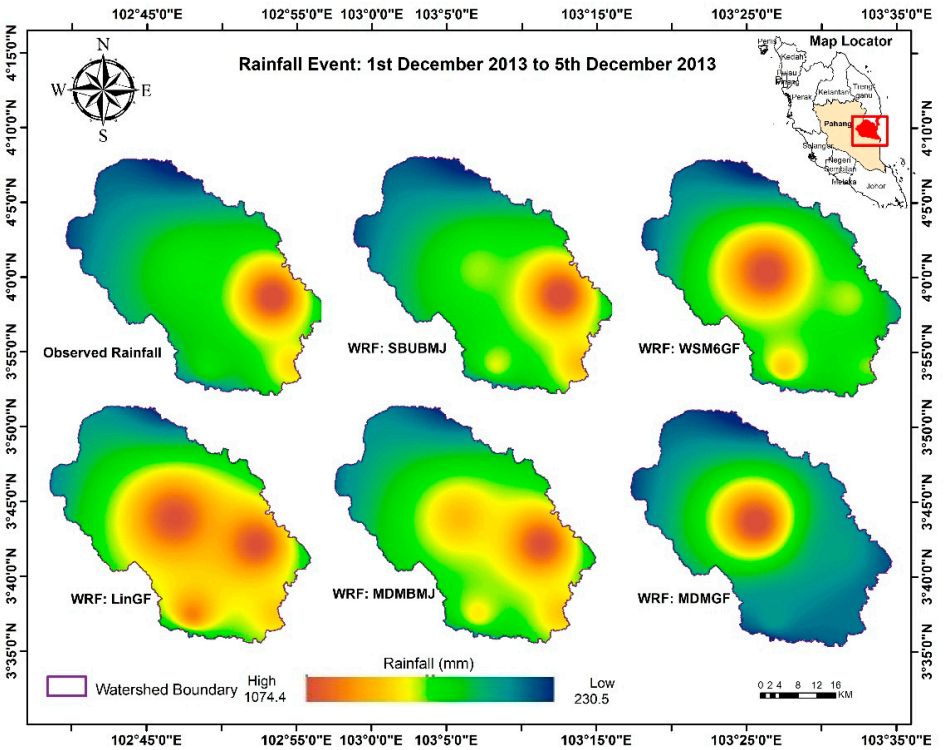

Figure 17. Spatial rainfall pattern for event from 1 to 5 December 2013 in KRB.

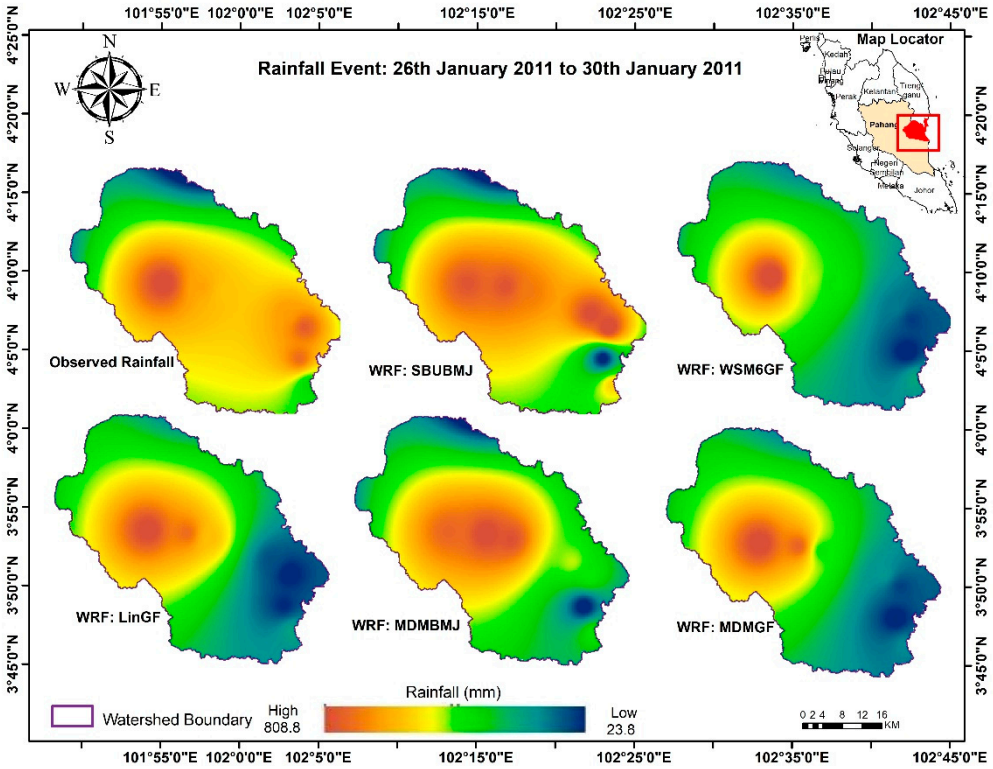

Figure 18. Spatial rainfall pattern for event from 26 to 30 January 2011 in KRB.

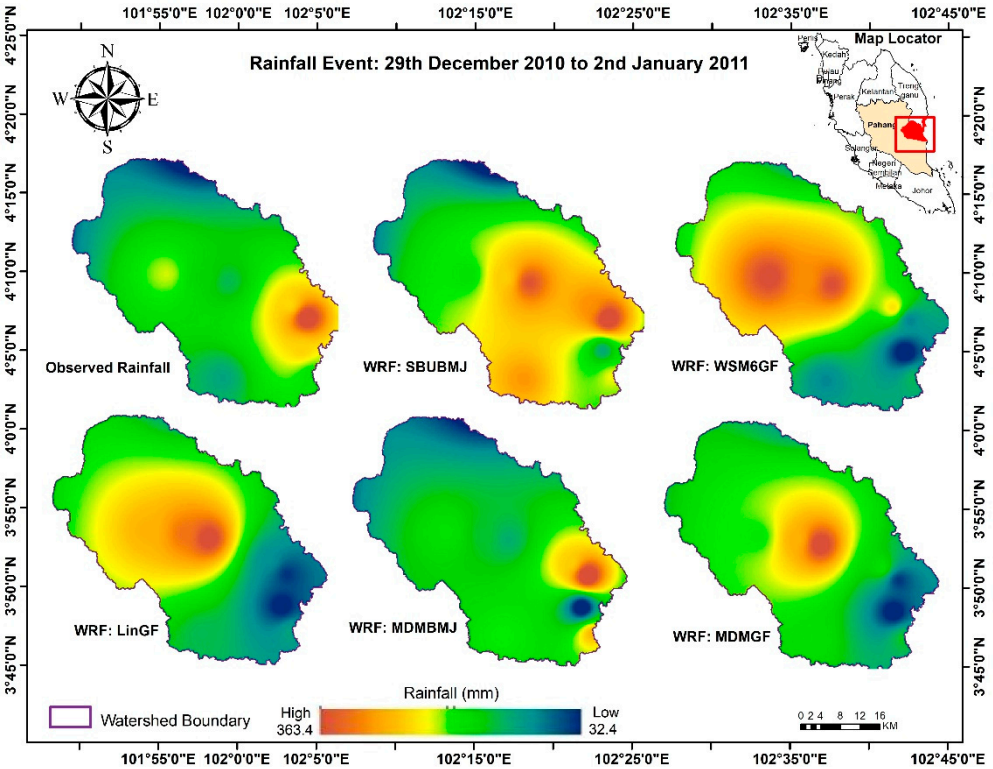

Figure 19. Spatial rainfall pattern for event from 29 December 2010 to 2 January 2011 in KRB.

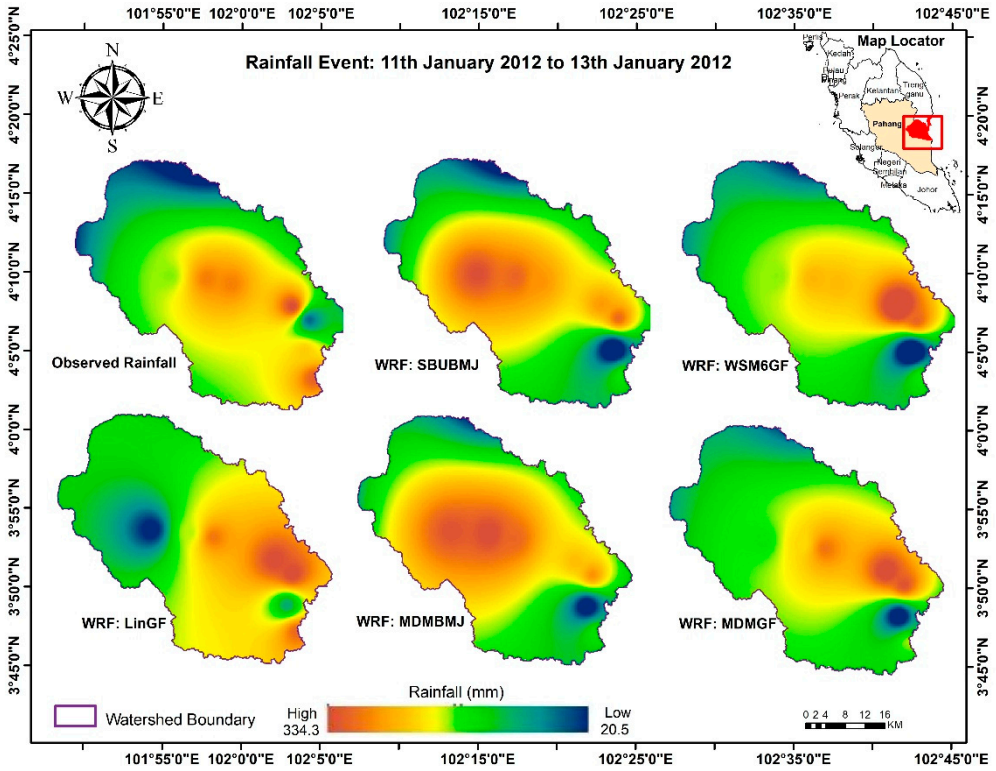

Figure 20. Spatial rainfall pattern for event from 11 to 13 January 2012 in KRB.

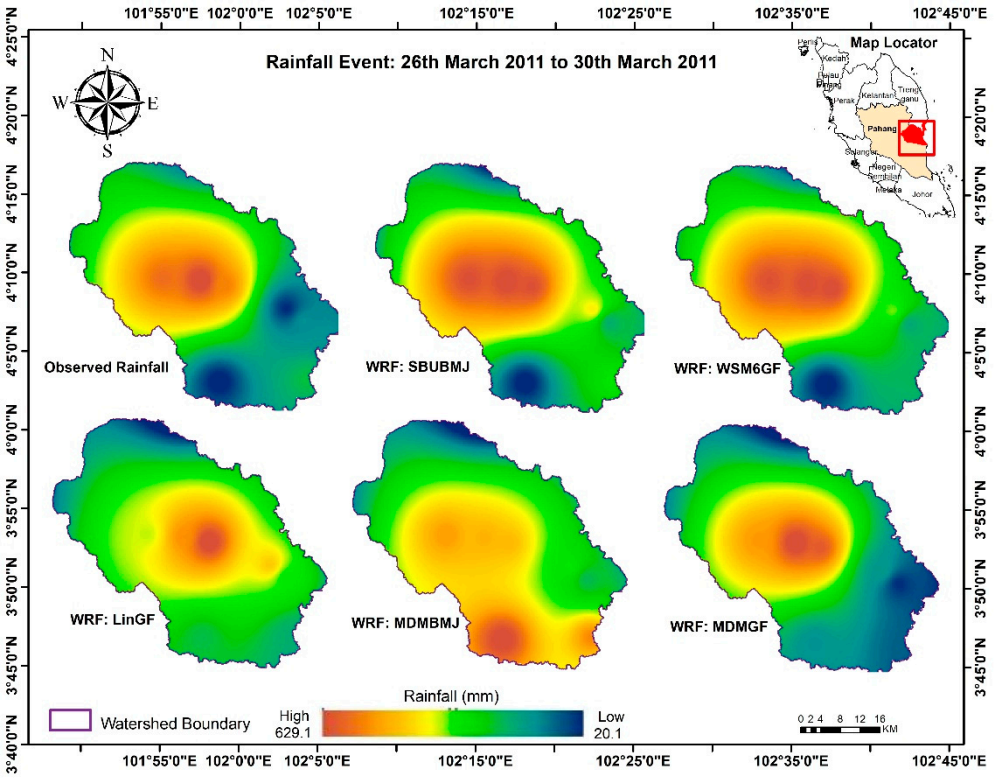

Figure 21. Spatial rainfall pattern for event from 26 to 30 March 2011.

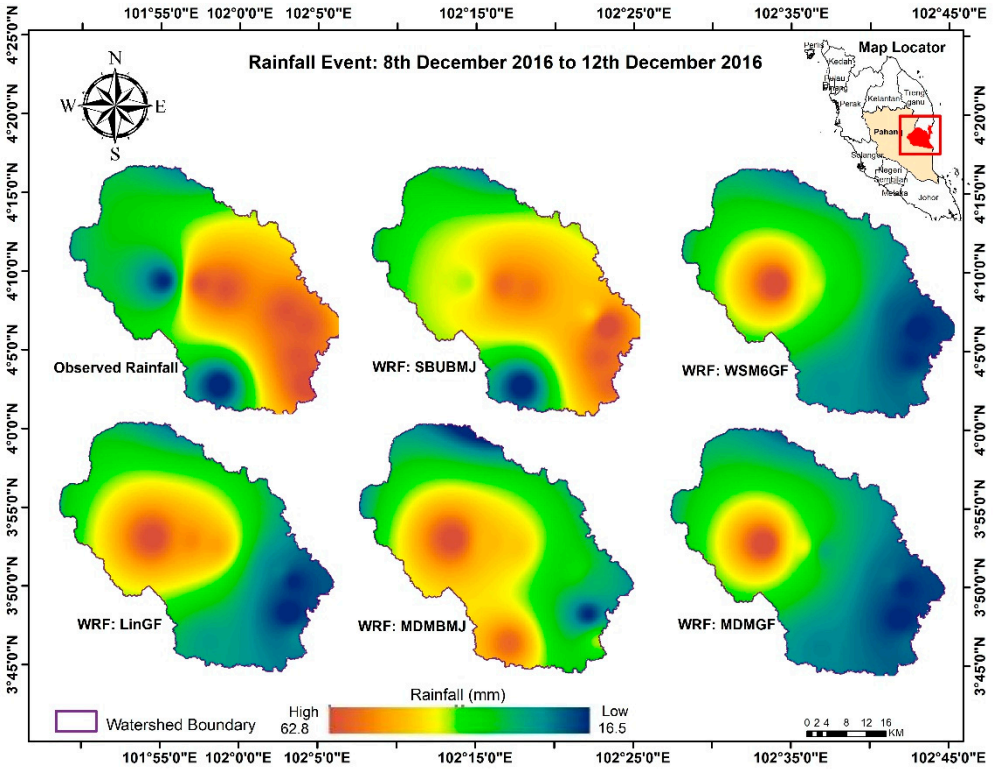

Figure 22. Spatial rainfall pattern for event from 8 to 12 December 2016 in KRB.

4. Discussion

In the first objective, a series of 48 experiments on the combinations of 8 microphysics and 6 cumulus schemes in WRF has been conducted to estimate the rainfall event that occurred from 29 December 2010 to 2 January 2012 at KRB. The results from the 4 km nested domain were used for all the analyses and comparisons. All the simulations were made for 3 and 5 days. Comparisons between the WRF scheme's estimated rainfall and the observed rainfall are shown in Figures 4–8. It has been noted that there was a considerable variation in the scheme's simulated results against the observed data. This could be due to the variation in atmospheric properties and topographic characteristics at certain stations and the non-suitability of domain configuration.

The results indicated that most of the schemes were not able to produce significant rainfall magnitude for all events. However, in the parameterized case, GF and BMJ cumulus schemes and SBU microphysics schemes are found to be relatively better to simulate the events (for example, WSM6GF, GoMGF, SBUGF, SBUBMJ, WSM6BMJ, and MDMBMJ). The identification of best-performing combinations was achieved by using categorical statistical evaluation techniques. These techniques were PC, TS, HR, FAR, Bias, and continuous indices (RMSE). An average, a lower RMSE of 41.8 identified that the BMJ cumulus scheme could simulate the event with a better scope. In KRB, the average values of the PC range from 0.61 to 0.67 and TS ranges from 0.55 to 0.67 reveal the parameterization of BMJ and GF (cumulus schemes) with MDM, SBU, WSM6, and Lin (microphysics schemes) perform relatively better to estimate the rainfall.

The Bias values revealed that BMJ cumulus parameterization tends to produce a slightly overestimated amount of rainfall. FAR and HR for the specific MP and CU schemes combination in the KRB area are less sensitive, as almost all the model combinations produced the rain. The reason could be that the area receives rainfall almost every day during the NEM season, therefore, there is no chance for both schemes (MP and CU) to miss the rainfall simulation. Performance of BMJ, KF, and GF (cumulus schemes) and SBU and MDM (microphysics schemes) is noticeably competent in terms of HR. The combination of WSM6KF has been identified as comparatively weaker than others in producing FAR.

Overall analysis reveals that the BMJ and GF schemes from cumulus and SBU, and MDM schemes from microphysics, are superior to providing reliable simulation results. The reliability of the results for cumulus schemes is supported by previous studies. Refs. [34,50] found the BMJ scheme's potential to produce promising results in simulating convective type rain in Malaysia; however, the suitability of the scheme's performance is case dependent. Further results similar to this study have been found for other regions, for instance, Ref. [51] compared BMJ, KF, and GF schemes by simulating monsoon rainfall over the Indian region and determined that BMJ schemes produced more realistic rainfall prediction compared with the observed data. Similarly, the sensitivity of the convective scheme parameterization was tested by [52] for simulation of a meso-convective system (see Table 16). The study determined that the BMJ scheme contributed significantly to capturing the convective storm. The fact could be that the rainfall in the tropical regions including Malaysia is produced from convective systems. The BMJ scheme in a convective system has the characteristics to adjust the temperature and moisture profiles into the atmosphere, which are in a quasi-equilibrium state in deep and shallow convection.

The microphysics schemes contain the explicit resolved processes of water vapor, clouds, and rainfall; thus, the scheme has a vital role in weather forecasting. However, there is not much research in evaluating the performance of microphysics schemes for Malaysia that has been documented. The performance of these schemes has been assessed in other regions including the middle latitude region [53], western Canada [54], southeast India [55], and the Shasta Dam watershed, northern California [56]. This study analysis determines that the microphysics schemes SBU and MDM showed significant performance when combined with the other cumulus schemes. The reason might be the properties of prognostics hydrometeor species that play a larger role in high-resolution WRF simulation for the squall lines case associated with convective or heavy precipitation. It must be emphasized that the sensitivity of microphysics should be tested for the different scenarios.

Table 16. Comparative results of similar studies in simulating rainfall.

Region and Reference	Microphysics (MP)	Cumulus (CU)	Results
South China Sea [57]	WRF Single Moment—3 class Eta New Thompson Stony Brook University Lin Scheme	Kain–Fritsch Betts–Miller–Janjic NewSimplified Arakawa Tiedtke	Overall, the WRF model schemes combination have an acceptable performance to predict important parameters (winds, rainfall) related to typhoon. However, the best estimated precipitation rate was identify with constantly lowest RMSE, MBE, and t values and highest CE values, 0.00025, 0.00015, 3.699,and 0.405, repectively.
Eastern Peninsular Malasysia (using MM5) [50]	-	Kain–Fritsch Betts–Miller Grell Anthes–Kuo	**Betts–Miller** performed better compared with obverserd TRMM rainfall with least RMSE (0.54, 1.2, 0.65), systematic RMSE (0.44, 1.04, 0.58), and unsystematic RMSE (0.31, 0.42, 0.30) at 06z09, 00z10, and 18z10 (6 hr interval), repectively
Ganges–Brahmaputra–Meghna basin (GBMB) and, Indus Basin (IB) [51]	WRF Single Moment—3 WRF Single Moment—5 WRF Single Moment—6 class Thompson Scheme	Kain–Fritsch Betts–Miller–Janjic Grell–Freitas	Combination of MPCU **WSM-5-BMJ** showed better consistant performance in all conditions at both regions. The approximate estimated POD, CSI, FBI, and FAR, TOPSIS-RSV were reported as 0.8, 0.6, 0.9–1.2, 0.2–0.3, and 0.7–0.8, respectively.
Southeast India [52]	Lin Scheme Thompson WRF Single Moment—6 class	Betts–Miller–Janjic Kain–Fritsch-Grell–Devenyi	Compared with obsereved parameters, the meso-scale convetive system including wram temperature, refelectvity, and rainfall pattern are well simulated by WRF schemes **MP Thompson, CU Betts–Miller–Janjic, and Mellor–Yamada–Janjic** PB layer with less RMSE (2.32, 1.01) and Bias (5.42, 1.04) and high correlation (0.74 T_{2m}, 0.19 h_{2m}, and ws_{10m}), respectively.
Chennai Southeast India [55]	Morrison double moment scheme Lin scheme WRF Single Moment—3 Class and 6 Class New Thompson scheme		**Morrison Double Moment (MDM)** schemes tend to perform better in simulating heavy rainfall events with estimated less RMSE 13.86, MAE, 11.03, and Bias 8.235.

It is important to note that this study evaluates the performances of the schemes by simulating one rainfall event (29 December 2010 to 2 January 2011), and it is difficult to interpret why the scheme performances are generally different. Therefore, it is required to simulate more events of different scenarios such as heavy, moderate, and extreme rainfall to validate the sensitivity of schemes' parameterization in the WRF model for KRB. The limitation of time and computational constraint was not allowed to evaluate all 48 schemes' combinations in simulating other rainfall events which have been selected for this research. Therefore, the top five efficient MP-CU schemes combinations, which were evaluated and ranked according to their performance through statistical methods, were selected to simulate other selected rainfall events. The purpose was to identify the best performing WRF parameterized physical schemes for KRB.

In the second phase, the selected five WRF parameterized MP, and CU schemes were tested for seven different rainfall events which were categorized into extreme, heavy, and moderate. Figures 9–15 display the simulated rainfall depth for all categorized events. The accumulated results indicated that all the schemes' parameterizations exhibit a considerable difference in the simulated amount of rainfall. From the close comparisons between the observed and WRF scheme's estimated rainfall depths, as shown in Tables 9–15, it has been observed that all the schemes' combinations produced varied estimations in all rainfall events. For the extreme and heavy rainfall events, the parameterization of WSM6GF, LinGF, and MDMGF showed lower prediction skills with a percentage error difference range from −47.3% to −87.2%, from −26.9% to −71.7%, and from −29.4% to −59.3%, respectively, whereas the PE (%) of these schemes, WSM6GF (164.7 and 547), LinGF (113.6 and 563), and MDMGF (139.1 and 564), showed the model produced a very high amount of rainfall depth compared to that observed in moderate rainfall events. Thus, the parameterization of these MP and CU schemes is found to not be compatible with simulating moderate rainfall events. On the other hand, the parameterized SBUBMJ schemes were identified as more reliable to simulate heavy and moderate rainfall events and have produced overpredicted and underpredicted rainfall with an average PE range from 17.5% to 25.2%. However, a PE ratio ranging from −58.1% to 68.2% in simulating extreme rainfall showed that schemes did not capture the event accurately. The uncertainty of WRF schemes' performances in producing rainfall in KRB is possibly due to the process of rainfall estimation which is based on various interactive factors and is challenging. These factors involve the behavior of domain configurations, topographical characteristics of an area, sparse rainfall data, and the absence of vertical-sounding observations.

Furthermore, the pattern spatial distribution of WRF simulated all seven rainfall events and was compared with the observed rainfall pattern. From the comparison, it has been noted that the parameterization of WRF MP and CU schemes produces comparable rainfall patterns in most of the model simulations. However, the combination of SBUBMJ schemes showed a more realistic performance in capturing the distributed rainfall pattern compared with the observed trend overall. Another possible reason for the varied performance of the scheme combinations could be the contribution of local boundary formulation in the Planetary Boundary Layer (PBL) condition, which seeks to capture and simulate the vertical environment. As the evaluation of PBL was not the scope of the research objective, therefore, this study used the default Yousei University (YSU) PBL condition in the WRF model configuration.

Moreover, it should be noted that the selection of the MP scheme has a greater influence on capturing the spatial pattern of rainfall distribution, and CU schemes influence capturing rainfall intensity in the model. In this regard, the SBU scheme from microphysics and BMJ from cumulus evolve in the potential configurations to simulate the spatial and temporal rainfall pattern for all the selected events in KRB. Considering the performance of BMJ cumulus schemes, the results are consistent with some previous studies, as discussed earlier. Ref. [51] evaluated the 15 combinations of MP and CU schemes to identify the suitable configuration of WRF model schemes in simulating Indian monsoon rainfall over the Ganges–Brahmaputra–Meghna River basins. The study used two nesting domains of 27 km

and 9 km grid resolutions, and the simulation results determined the BMJ cumulus as being superior to perform well when combined with the MP schemes' options of WSM3, WSM6, and Thompson. Similarly, ref. [58] invested different combinations of four microphysics, two cumulus, and two planetary boundary layers for simulating the extreme rainfall event at the upper Ganga Basin. The output of the study revealed that BMJ was the best configuration with microphysics Goddard (GoM) and Millor–Yamada–Janjis (MYJ) PBL to capture the event successfully.

According to [59], compared to other WRF cumulus schemes, the BMJ scheme shows more agreement to the ground observed in simulating stratiform and convective precipitations. The research attempted to assess the WRF's capability to simulate the flood event in Yorkshire–Humberside (UK) that occurred in 1999. In the case of microphysics (MP) schemes, there are minimal studies in comparison to configurations for simulated different storm events. Ref. [8] concluded that all the MP schemes are very influential in the rainfall simulation at high grid resolutions due to the impact of the water phase process. As for SBU microphysics performance, in the simulation of tropical rainfall events, there is not much research that has been conducted. To understand and analyze the behavior of SBU schemes' configuration over the Malaysian region, it is required to perform more simulation tests by using different storm conditions. From the overall analysis of WRF model schemes combinations, the study has identified the combination of SBUBMJ physical schemes in the WRF model to generate the meteorological data for the rainfall for hydrological simulation in KRB.

5. Conclusions

WRF model sensitivity was evaluated to simulate a 5-day rainfall period against the observed rainfall data using 48 different parameterized MP and CU schemes. All the parameterized schemes simulations show varied performance in estimating rainfall at different rainfall gauge locations at the studied basin. The statistical methods, including RMSE, PC, TS, HR, FAR, and Bias, were applied to analyze the accuracy of the simulations. Results obtained from the statistical indices have indicated varied performance levels for the combination of the physical schemes. The model schemes were ranked based on their performances in each index. Then, all the ranked values were combined to form cumulative rank orders. The obtained results indicate that parameterization of SBUBMJ, WSM6GF, LinGF, MDMBMJ, and MDMGF is found to be potentially significant to produce a good agreement with the observed data. To identify the most efficient parameterized physical schemes for KRB, sets of the selected five schemes combinations have been further investigated by simulating different rainfall events. Parameterization of MP Schemes WSM6, Lin, and MDM with CU GF schemes shows less accuracy in rainfall estimation compared to the observed rainfall, whereas the combination of CU scheme BMJ with MP schemes MDM and SBU shows relatively better results. Overall, however, it was found that the parameterization of Stony Brook University–Betts–Miller–Janjic (SBUBMJ) resulted in a good agreement in capturing both spatial and temporal rainfall patterns that can be used in the hydrological simulation, especially in cases of heavy and moderate rainfall with the PE range from $\pm$17.5%to $\pm$25.2%. However, it produced uncertainty in simulating extreme rainfall events with estimated PE ranges from $\pm$58.1% to $\pm$68.2%. It is, therefore, required to test the parametrization SBUBMJ with different boundary layer conditions and domain configurations for simulating extreme rainfall more accurately. In the conclusion, the findings in this study indicate that for the region where hydro-meteorological data are limited or incomplete, the alternative approach can be used to establish more sustainable and reliable hydrological forecasting utilizing the WRF model. This is important in ensuring sustainable water resource management and monitoring in the data-scarce region.

Author Contributions: Conceptualization, S.M.Z. and J.I.A.G.; data curation, S.M.Z., J.I.A.G., S.M. and S.K.N.; formal analysis, S.M.Z. and M.E.; funding acquisition, J.I.A.G. and Q.Y.; investigation, S.M.Z. and J.I.A.G.; methodology, S.M.Z. and J.I.A.G.; project administration, S.M.Z. and Q.Y.; resources, S.M.Z. and S.M.; software, S.M.Z. and M.E.; supervision, J.I.A.G.; validation, Q.Y. and

S.K.N.; visualization, S.M.Z., J.I.A.G. and M.E.; writing—original draft, S.M.Z.; writing—review and editing, S.M.Z., J.I.A.G., M.E., Q.Y., S.M. and S.K.N. All authors have read and agreed to the published version of the manuscript.

Funding: This research was funded by the Ministry of Higher Education Malaysia, grant number FRGS/1/2021/WAB02/UMP/02/2 (University reference: RDU210120), and Universiti Malaysia Pahang, grant number UIC221507. The APC was funded by the National Natural Science Foundation of China, grant number 51909273, and Program for the Introduction of High-End Foreign Experts, grant number G2021058002L.

Institutional Review Board Statement: Not applicable.

Informed Consent Statement: Not applicable.

Data Availability Statement: The authors would like to collaborate, and data can be made available upon request. Some data are confidential in the region and distribution is prohibited.

Acknowledgments: The authors would like to express their gratitude to the Department of Irrigation and Drainage Malaysia and the Malaysian Meteorological Department for providing the hydrological and climate data for this research. Additionally, the authors are very grateful for all the technical supports including filed survey, manpower, analysis works, proof reading service, and funding provided by the University Malaysia Pahang, Balochistan University of Engineering and Technology Khuzdar, China Institute of Water Resources and Hydropower Research, Institute of Bio-Geosciences Research Juelich Germany, and University of Bonn.

Conflicts of Interest: The authors declare no conflict of interest.

Appendix A

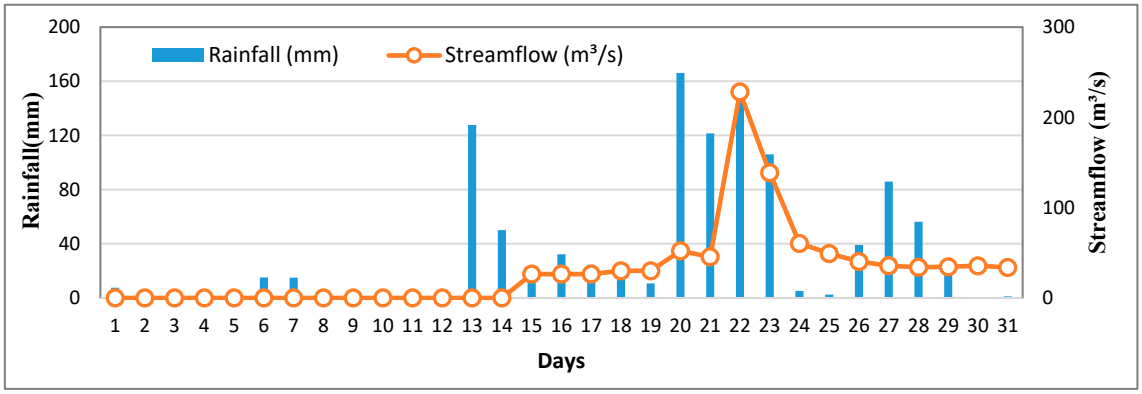

Figure A1. Daily average rainfall and streamflow for December 2001.

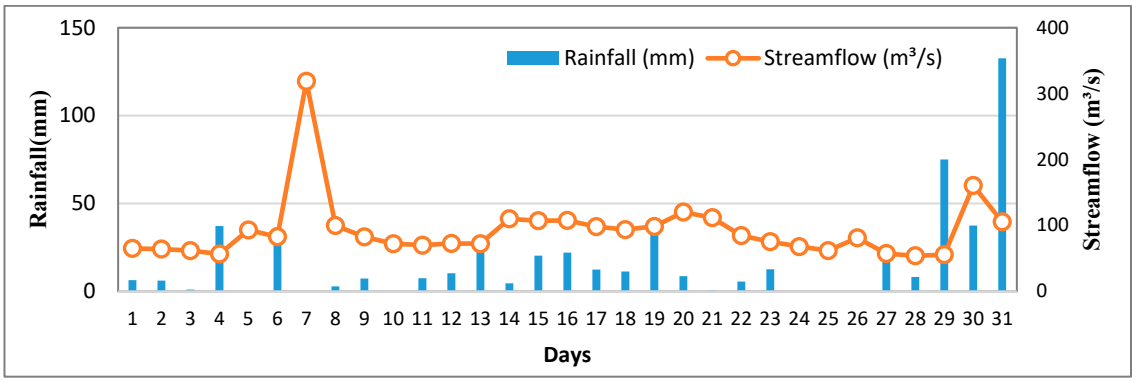

Figure A2. Daily average rainfall and streamflow for December 2010.

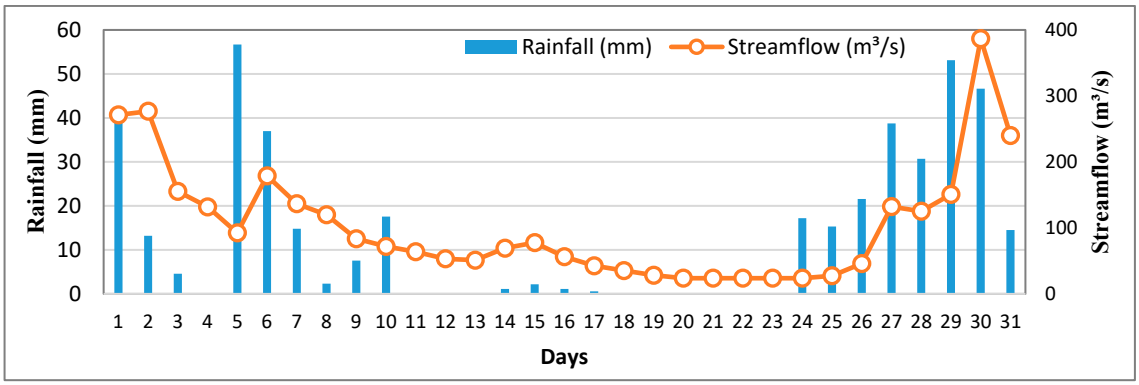

Figure A3. Daily average rainfall and streamflow for January 2011.

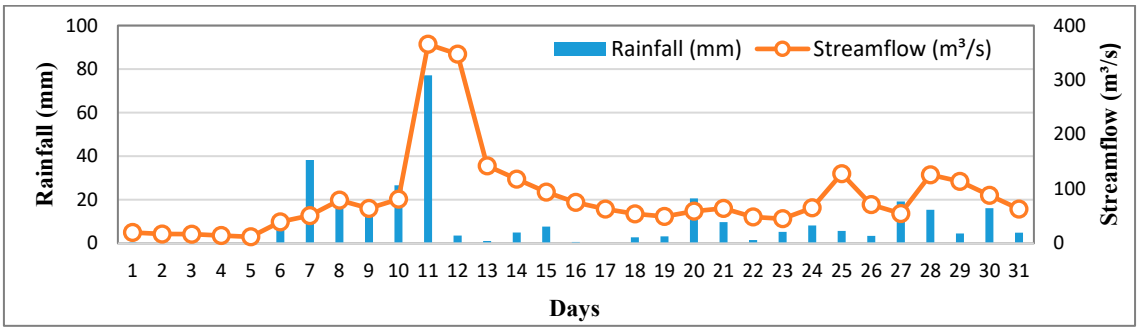

Figure A4. Daily average rainfall and streamflow for March 2011.

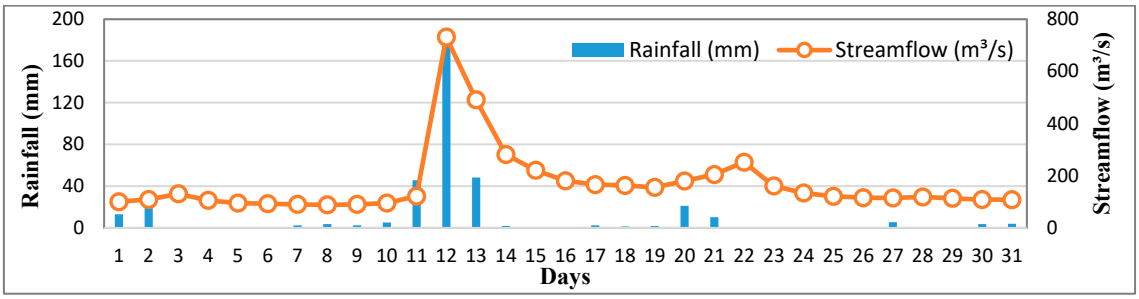

Figure A5. Daily average rainfall and streamflow for January 2012.

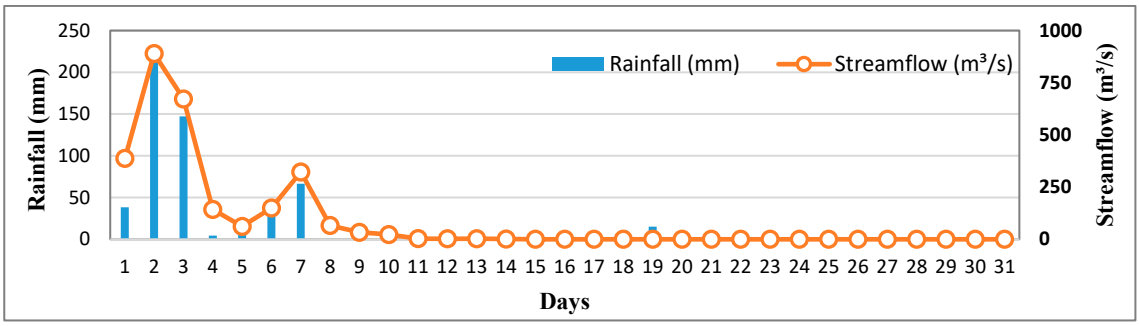

Figure A6. Daily average rainfall and streamflow for December 2013.

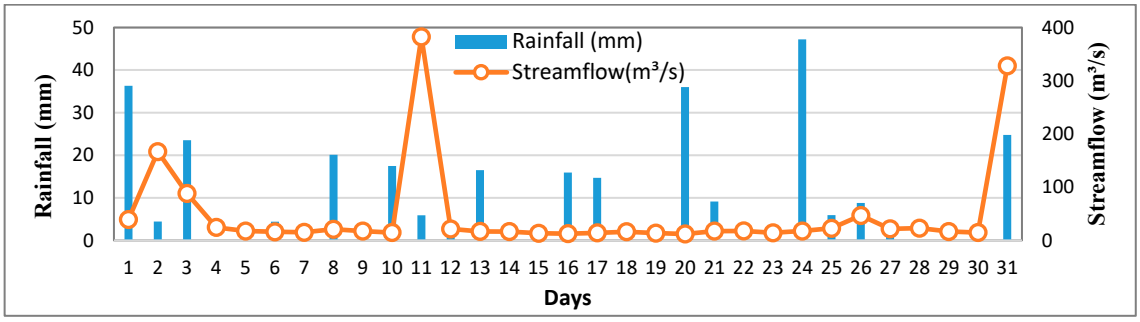

Figure A7. Daily average rainfall and streamflow for December 2016.

Table A1. RMSE (mm) of WRF physical schemes combination at rainfall stations of KRB.

Schemes name	Kg.Sg. Soi	Pulau Manis	Paya Besar	PCCL Lembing	Rumah Pam	JKR Gamabang	Ladang Nada	Ladang Kuala Raman	JPS Negeri Pahang	R 1	R 2	R 3	R 4	R 5	R 6	R7	R8	R 9	Total	All Ranked
KSKF	34	34	54	70	49	32	58	47	73	20	21	18	29	11	21	33	20	9	182	19
KSBMJ	33	36	55	74	53	34	58	50	80	19	28	23	43	19	25	34	40	24	255	27
KSGF	26	25	52	76	45	25	35	30	76	4	2	10	44	6	2	2	2	17	89	6
KSG3D	39	38	57	70	55	35	57	47	81	33	38	33	31	24	34	26	21	29	269	31
KSTiS	33	33	52	69	50	30	54	43	76	16	17	11	22	16	16	15	12	16	141	13
KSOKF	37	37	55	76	49	34	67	52	73	27	30	22	45	13	30	45	41	10	263	28
LinKF	39	36	58	71	60	34	58	50	84	37	25	37	38	42	29	40	38	42	328	38
LinBMJ	31	38	55	77	53	34	73	62	75	11	35	20	46	20	28	46	44	14	264	29
LinGF	32	28	55	60	52	27	31	27	80	13	6	21	3	17	5	1	1	23	90	7
LinG3D	41	38	58	70	59	36	57	49	83	42	44	42	30	36	43	30	32	34	333	39
LinTiS	37	35	54	67	56	33	54	45	82	30	23	15	15	28	24	13	15	31	194	20
LinOKF	39	38	58	70	54	35	58	47	81	34	36	36	35	22	33	35	23	27	281	35
WSM3KF	41	39	59	71	61	36	59	50	85	48	45	48	40	45	45	42	39	47	399	48
WSM3BMJ	36	35	55	67	55	32	54	44	80	23	22	19	16	23	20	16	13	22	174	17
WSM3GF	33	29	55	49	56	28	52	41	83	17	8	25	2	26	9	9	4	36	136	12
WSM3G3D	41	39	58	70	59	36	57	48	83	47	46	47	28	34	46	32	29	38	347	44
WSM3TiS	41	38	57	69	58	36	56	48	83	43	43	30	24	32	38	21	27	40	298	36
WSM3OKF	41	39	58	71	57	36	58	49	81	46	47	41	37	29	44	38	30	26	338	41
WSM6KF	40	38	58	71	60	35	58	50	84	38	34	40	39	41	36	41	37	44	350	45
WSM6BMJ	34	37	57	68	60	60	57	48	84	21	29	29	18	38	48	25	25	43	276	32
WSM6GF	30	27	53	72	41	27	56	43	73	9	4	13	41	4	6	19	11	11	118	11
WSM6G3D	39	38	57	70	55	35	57	48	80	35	37	35	34	25	37	28	24	21	276	33
WSM6TiS	38	36	55	69	56	34	56	46	81	31	26	26	27	27	26	20	18	28	229	24
WSM6OKF	37	37	58	70	57	35	57	48	81	28	31	38	32	30	32	29	26	30	276	34
GoMKF	34	32	49	64	52	30	51	43	76	22	16	3	8	18	15	5	10	15	112	10
GoMBMJ	37	44	57	74	67	41	63	58	96	26	48	32	42	48	47	43	43	48	377	47
GoMGF	27	29	49	168	64	32	164	119	79	6	9	4	48	47	23	48	48	20	253	26
GoMG3D	24	28	50	65	39	28	54	44	62	3	5	5	10	3	8	14	14	2	64	3
GoMTiS	31	30	51	63	53	30	50	41	77	10	12	6	6	21	14	4	6	18	97	8
GoMOKF	37	33	57	64	58	31	53	46	82	29	18	31	7	33	19	11	17	32	197	22
NThKF	39	36	57	69	59	34	56	47	83	32	27	34	26	35	27	22	22	39	264	30
NThBMJ	29	29	53	61	48	27	47	37	72	8	11	12	4	8	4	3	3	8	61	2
NThGF	29	25	52	48	43	26	51	58	71	7	3	9	1	5	3	7	42	7	84	5
NThG3D	40	38	58	69	60	35	57	49	82	39	33	39	23	40	35	27	35	33	304	37
NThTiS	36	34	55	66	50	31	53	42	77	25	19	24	13	14	18	10	8	19	150	15
NThOKF	41	38	58	70	59	36	58	49	83	41	42	43	33	37	39	36	31	37	339	42
MDMKF	41	38	58	68	60	36	57	49	84	44	40	45	20	43	41	23	33	45	334	40
MDMBMJ	27	31	51	64	49	29	51	42	71	5	13	7	9	9	10	6	7	6	72	4
MDMGF	32	29	54	65	63	30	66	73	80	12	7	14	11	46	13	44	45	25	217	23
MDMG3D	41	38	58	68	60	36	57	49	84	45	41	46	21	44	42	24	34	46	343	43
MDMTiS	39	38	56	68	57	35	54	45	83	36	32	28	17	31	31	18	16	35	244	25
MDMOKF	41	38	58	70	60	36	58	49	83	40	39	44	36	39	40	37	36	41	352	46
SBUKF	32	31	54	67	49	29	54	74	43	14	14	16	14	10	11	17	46	1	143	14

Table A1. *Cont.*

Schemes name	Kg.Sg. Soi	Pulau Manis	Paya Besar	PCCL Lembing	Rumah Pam	JKR Gamabang	Ladang Nada	Ladang Kuala Raman	JPS Negeri Pahang	R 1	R 2	R 3	R 4	R 5	R 6	R7	R8	R 9	Total	All Ranked
SBUBMJ	21	29	45	62	36	27	51	41	63	2	10	1	5	1	7	8	5	3	42	1
SBUGF	20	21	47	125	37	24	127	104	64	1	1	2	47	2	1	47	47	4	152	16
SBUG3D	36	34	56	69	50	32	57	47	75	24	20	27	25	15	22	31	19	13	196	21
SBUTiS	33	31	52	66	49	30	54	42	74	15	15	8	12	12	12	12	9	12	107	9
SBUOKF	33	36	54	68	46	30	58	48	71	18	24	17	19	7	17	39	28	5	174	18

Table A2. Cumulative ranking for WRF schemes combination.

Schemes	PC	HR	FAR	TS	RMSE	BIAS	Total	Cumulative Rank
KSKF	29	33	4	34	19	14	133	21
KSBMJ	26	30	3	29	27	13	128	18
KSGF	18	15	34	17	6	31	121	16
KSG3D	47	45	45	43	31	4	215	45
KSTiS	34	37	19	36	13	11	150	29
KSOKF	40	48	1	48	28	1	166	31
LinKF	48	40	48	45	38	9	228	48
LinBMJ	16	21	12	16	29	29	123	17
LinGF	5	18	2	13	7	26	71	3
LinG3D	46	42	42	42	39	8	219	47
LinTiS	30	29	21	30	20	17	147	28
LinOKF	39	43	17	40	35	6	180	35
WSM3KF	45	44	10	44	48	5	196	38
WSM3BMJ	20	28	6	25	17	22	118	13
WSM3GF	17	20	14	21	12	30	114	12
WSM3G3D	42	46	32	46	44	3	213	43
WSM3TiS	41	41	30	41	36	7	196	39
WSM3OKF	43	47	20	47	41	2	200	41
WSM6KF	37	35	46	35	45	20	218	46
WSM6BMJ	22	22	18	23	32	27	144	26
WSM6GF	3	10	5	8	11	32	69	2
WSM6G3D	44	39	47	39	33	12	214	44
WSM6TiS	36	36	44	37	24	19	196	40
WSM6OKF	23	24	11	26	34	21	139	25
GoMKF	10	5	41	6	10	46	118	14
GoMBMJ	12	11	15	12	47	39	136	23
GoMGF	6	6	27	4	26	43	112	10
GoMG3D	15	12	29	15	3	38	112	11
GoMTiS	19	16	33	18	8	35	129	19
GoMOKF	9	9	9	9	22	40	98	8
NThKF	25	19	39	20	30	34	167	32
NThBMJ	7	7	31	7	2	44	98	9
NThGF	13	14	13	14	5	37	96	6
NThG3D	38	38	24	38	37	10	185	36
NThTiS	31	32	8	31	15	15	132	20
NThOKF	24	23	23	22	42	28	162	30
MDMKF	33	31	35	32	40	16	187	37
MDMBMJ	2	2	28	2	4	48	86	4
MDMGF	8	13	7	10	23	33	94	5
MDMG3D	35	34	37	33	43	18	200	42
MDMTiS	28	26	16	27	25	23	145	27
MDMOKF	27	25	26	24	46	25	173	33
SBUKF	11	3	38	5	14	47	118	15
SBUBMJ	1	1	22	1	1	41	67	1
SBUGF	4	4	25	3	16	45	97	7
SBUG3D	32	27	43	28	21	24	175	34
SBUTiS	21	17	36	19	9	36	138	24
SBUOKF	14	8	40	11	18	42	133	22

Table A3. Percentage of correction (PC).

Sch-Name	Kg.Sg. Soi	Pulau Manis	Paya Besar	PCCL Sg. Lembing	Rumah Pam	JKR Gambang	Ldn Nada	Ldn Kuala Raman	JPS Negeri Pahang
KSKF	0.74	0.68	0.66	0.34	0.34	0.60	0.41	0.42	0.74
KSBMJ	0.75	0.68	0.69	0.37	0.38	0.62	0.41	0.39	0.75
KSGF	0.78	0.69	0.71	0.33	0.46	0.64	0.45	0.45	0.78
KSG3D	0.57	0.63	0.44	0.31	0.26	0.53	0.33	0.37	0.57
KSTiS	0.68	0.59	0.69	0.31	0.40	0.56	0.41	0.40	0.68
KSOKF	0.61	0.60	0.55	0.31	0.29	0.62	0.33	0.35	0.61
LinKF	0.68	0.63	0.55	0.15	0.23	0.53	0.24	0.24	0.68
LinBMJ	0.79	0.74	0.60	0.45	0.52	0.63	0.47	0.40	0.79
LinGF	0.81	0.69	0.76	0.49	0.50	0.68	0.61	0.57	0.81
LinG3D	0.73	0.60	0.45	0.31	0.25	0.56	0.32	0.33	0.73
LinTiS	0.73	0.61	0.70	0.40	0.36	0.57	0.44	0.43	0.73
LinOKF	0.71	0.62	0.57	0.32	0.24	0.60	0.34	0.35	0.71
WSM3KF	0.70	0.64	0.56	0.24	0.26	0.56	0.27	0.29	0.70
WSM3BMJ	0.76	0.71	0.69	0.38	0.45	0.60	0.41	0.44	0.76
WSM3GF	0.74	0.68	0.70	0.46	0.48	0.60	0.54	0.55	0.74
WSM3G3D	0.62	0.59	0.48	0.36	0.26	0.55	0.35	0.38	0.62
WSM3TiS	0.65	0.52	0.64	0.31	0.33	0.52	0.35	0.35	0.65
WSM3OKF	0.63	0.60	0.51	0.33	0.27	0.59	0.30	0.33	0.63
WSM6KF	0.75	0.69	0.60	0.19	0.33	0.60	0.23	0.26	0.75
WSM6BMJ	0.74	0.69	0.64	0.40	0.50	0.58	0.48	0.42	0.74
WSM6GF	0.86	0.69	0.80	0.47	0.58	0.69	0.58	0.59	0.86
WSM6G3D	0.64	0.61	0.49	0.22	0.30	0.55	0.31	0.35	0.64
WSM6TiS	0.70	0.59	0.68	0.34	0.35	0.57	0.35	0.35	0.70
WSM6OKF	0.78	0.76	0.64	0.42	0.31	0.60	0.46	0.44	0.78
GoMKF	0.74	0.68	0.69	0.68	0.76	0.60	0.74	0.65	0.74
GoMMBJ	0.82	0.69	0.67	0.48	0.60	0.64	0.54	0.45	0.82
GoMGF	0.78	0.70	0.76	0.57	0.55	0.63	0.64	0.61	0.78
GoMG3D	0.78	0.66	0.74	0.49	0.49	0.62	0.53	0.54	0.78
GoMTiS	0.74	0.60	0.70	0.50	0.60	0.58	0.52	0.54	0.74
GoMOKF	0.78	0.74	0.76	0.50	0.37	0.66	0.57	0.54	0.78
NThKF	0.79	0.72	0.66	0.31	0.47	0.64	0.36	0.35	0.79
NThBMJ	0.76	0.69	0.72	0.55	0.62	0.62	0.60	0.55	0.76
NThGF	0.82	0.64	0.70	0.49	0.52	0.64	0.55	0.55	0.82
NThG3D	0.74	0.66	0.45	0.31	0.26	0.60	0.35	0.36	0.74
NThTiS	0.74	0.59	0.70	0.44	0.39	0.56	0.45	0.44	0.74
NThOKF	0.82	0.73	0.61	0.32	0.37	0.67	0.38	0.34	0.82
MDMKF	0.74	0.66	0.47	0.38	0.28	0.61	0.37	0.42	0.74
MDMBMJ	0.77	0.72	0.69	0.59	0.74	0.64	0.60	0.59	0.77
MDMGF	0.79	0.69	0.72	0.50	0.51	0.70	0.58	0.61	0.79
MDMG3D	0.74	0.66	0.47	0.39	0.28	0.61	0.37	0.42	0.74
MDMTiS	0.74	0.63	0.63	0.46	0.45	0.60	0.44	0.49	0.74
MDMOKF	0.79	0.69	0.65	0.31	0.40	0.69	0.35	0.34	0.79
SBUKF	0.77	0.73	0.69	0.43	0.67	0.64	0.55	0.53	0.77
SBUBMJ	0.77	0.73	0.74	0.66	0.60	0.65	0.68	0.63	0.77
SBUGF	0.78	0.71	0.68	0.58	0.53	0.65	0.64	0.64	0.78
SBUG3D	0.73	0.67	0.49	0.40	0.34	0.60	0.42	0.43	0.73
SBUTiS	0.74	0.64	0.69	0.50	0.59	0.60	0.47	0.51	0.74
SBUOKF	0.79	0.61	0.70	0.52	0.61	0.64	0.59	0.54	0.79

Table A4. Threat Score (TS).

Sch-Name	Kg.Sg. Soi	Pulau Manis	Paya Basar	PCCL Sg. Lembing	Rumah Pam	JKR Gamabng	Ldn Nada	Ldn Kuala Raman	JPS Negeri Pahang
KSKF	0.72	0.67	0.61	0.15	0.16	0.59	0.20	0.20	0.14
KSBMJ	0.73	0.66	0.64	0.19	0.23	0.59	0.20	0.20	0.17
KSGF	0.77	0.69	0.68	0.27	0.37	0.63	0.36	0.36	0.30
KSG3D	0.52	0.60	0.30	0.17	0.08	0.46	0.20	0.22	0.07
KSTiS	0.65	0.57	0.60	0.17	0.28	0.52	0.24	0.23	0.28
KSOKF	0.54	0.54	0.35	0.10	0.09	0.52	0.10	0.10	0.08
LinKF	0.66	0.63	0.47	0.01	0.07	0.52	0.04	0.02	0.08
LinBMJ	0.77	0.72	0.55	0.35	0.44	0.61	0.37	0.33	0.41
LinGF	0.79	0.68	0.72	0.41	0.40	0.65	0.53	0.47	0.29
LinG3D	0.70	0.59	0.35	0.18	0.05	0.54	0.20	0.17	0.05
LinTiS	0.71	0.61	0.64	0.25	0.24	0.56	0.27	0.27	0.24
LinOKF	0.67	0.60	0.46	0.15	0.08	0.56	0.14	0.14	0.07
WSM3KF	0.68	0.64	0.48	0.01	0.06	0.54	0.01	0.01	0.05
WSM3BMJ	0.73	0.68	0.62	0.26	0.34	0.57	0.28	0.29	0.34
WSM3GF	0.72	0.67	0.66	0.40	0.38	0.59	0.46	0.47	0.37
WSM3G3D	0.57	0.57	0.34	0.20	0.07	0.50	0.19	0.19	0.07
WSM3TiS	0.61	0.50	0.52	0.15	0.17	0.47	0.16	0.14	0.16
WSM3OKF	0.58	0.55	0.40	0.15	0.10	0.52	0.10	0.12	0.11
WSM6KF	0.74	0.69	0.55	0.00	0.17	0.59	0.01	0.02	0.12
WSM6BMJ	0.71	0.67	0.59	0.29	0.42	0.56	0.36	0.32	0.44
WSM6GF	0.84	0.68	0.75	0.41	0.49	0.67	0.50	0.49	0.34
WSM6G3D	0.63	0.61	0.38	0.11	0.10	0.53	0.19	0.21	0.14
WSM6TiS	0.69	0.59	0.62	0.19	0.22	0.56	0.20	0.18	0.24
WSM6OKF	0.77	0.75	0.54	0.29	0.15	0.56	0.32	0.29	0.20
GoMKF	0.74	0.68	0.68	0.68	0.75	0.60	0.73	0.65	0.79
GoMMBJ	0.81	0.69	0.63	0.41	0.51	0.63	0.46	0.37	0.43
GoMGF	0.77	0.70	0.74	0.54	0.51	0.63	0.58	0.55	0.37
GoMG3D	0.76	0.66	0.70	0.44	0.40	0.61	0.46	0.46	0.35
GoMTiS	0.73	0.60	0.67	0.45	0.53	0.57	0.46	0.45	0.50
GoMOKF	0.77	0.73	0.73	0.43	0.32	0.65	0.49	0.45	0.44
NThKF	0.78	0.72	0.61	0.27	0.38	0.63	0.27	0.25	0.34
NThBMJ	0.75	0.69	0.69	0.51	0.57	0.62	0.54	0.50	0.66
NThGF	0.80	0.64	0.67	0.42	0.44	0.63	0.47	0.46	0.40
NThG3D	0.72	0.66	0.35	0.19	0.06	0.58	0.22	0.21	0.05
NThTiS	0.71	0.59	0.63	0.31	0.22	0.54	0.29	0.27	0.19
NThOKF	0.79	0.72	0.53	0.24	0.25	0.65	0.26	0.22	0.25
MDMKF	0.72	0.65	0.38	0.25	0.11	0.59	0.27	0.29	0.09
MDMBMJ	0.76	0.72	0.68	0.56	0.71	0.64	0.57	0.55	0.65
MDMGF	0.78	0.68	0.68	0.42	0.42	0.68	0.49	0.50	0.32
MDMG3D	0.72	0.65	0.37	0.26	0.11	0.59	0.27	0.29	0.09
MDMTiS	0.72	0.63	0.55	0.32	0.32	0.59	0.31	0.35	0.25
MDMOKF	0.76	0.69	0.58	0.22	0.29	0.66	0.22	0.22	0.29
SBUKF	0.76	0.73	0.68	0.42	0.63	0.64	0.51	0.49	0.55
SBUBMJ	0.76	0.73	0.71	0.63	0.59	0.65	0.64	0.59	0.67
SBUGF	0.77	0.71	0.65	0.56	0.48	0.65	0.60	0.58	0.50
SBUG3D	0.71	0.67	0.42	0.31	0.18	0.59	0.33	0.31	0.15
SBUTiS	0.72	0.64	0.66	0.43	0.51	0.59	0.40	0.42	0.39
SBUOKF	0.78	0.60	0.66	0.50	0.58	0.64	0.55	0.50	0.54

Table A5. Hit Rate (HR).

Sch-Name	Kg.Sg. Soi	Pulau Manis	Paya Basar	PCCL Sg. Lembing	Rumah Pam	JKR Gamabng	Ldn Nada	Ldn Kuala Raman	JPS Negeri Pahang
KSKF	0.89	0.88	0.77	0.15	0.16	0.84	0.20	0.21	0.14
KSBMJ	0.90	0.84	0.79	0.19	0.23	0.83	0.20	0.22	0.18
KSGF	0.97	0.92	0.89	0.32	0.40	0.91	0.42	0.43	0.32
KSG3D	0.63	0.74	0.35	0.18	0.08	0.60	0.22	0.24	0.07
KSTiS	0.78	0.72	0.71	0.18	0.31	0.72	0.26	0.25	0.30
KSOKF	0.60	0.63	0.37	0.10	0.09	0.62	0.10	0.10	0.08
LinKF	0.85	0.84	0.59	0.01	0.07	0.77	0.04	0.02	0.08
LinBMJ	0.95	0.92	0.71	0.39	0.48	0.86	0.43	0.40	0.43
LinGF	0.92	0.86	0.88	0.46	0.42	0.88	0.58	0.53	0.31
LinG3D	0.84	0.78	0.43	0.19	0.05	0.75	0.22	0.20	0.05
LinTiS	0.87	0.81	0.78	0.26	0.25	0.80	0.28	0.29	0.26
LinOKF	0.78	0.76	0.55	0.16	0.08	0.75	0.15	0.15	0.07
WSM3KF	0.85	0.84	0.59	0.01	0.06	0.78	0.01	0.01	0.05
WSM3BMJ	0.87	0.84	0.74	0.28	0.36	0.78	0.30	0.32	0.35
WSM3GF	0.90	0.89	0.84	0.47	0.41	0.84	0.53	0.55	0.38
WSM3G3D	0.67	0.72	0.39	0.22	0.07	0.65	0.20	0.21	0.07
WSM3TiS	0.73	0.64	0.57	0.16	0.18	0.64	0.17	0.15	0.16
WSM3OKF	0.67	0.67	0.49	0.15	0.11	0.67	0.10	0.13	0.11
WSM6KF	0.95	0.92	0.74	0.00	0.18	0.88	0.01	0.02	0.13
WSM6BMJ	0.88	0.87	0.75	0.32	0.46	0.80	0.40	0.38	0.45
WSM6GF	0.99	0.90	0.89	0.48	0.52	0.94	0.56	0.56	0.36
WSM6G3D	0.81	0.81	0.46	0.13	0.10	0.75	0.22	0.24	0.14
WSM6TiS	0.89	0.79	0.77	0.20	0.23	0.80	0.22	0.20	0.26
WSM6OKF	0.97	0.98	0.62	0.30	0.16	0.78	0.34	0.32	0.22
GoMKF	0.96	0.91	0.96	0.88	0.93	0.90	0.96	0.90	0.96
GoMMBJ	1.00	0.93	0.83	0.47	0.55	0.93	0.54	0.45	0.45
GoMGF	0.99	0.94	0.93	0.64	0.61	0.94	0.69	0.67	0.42
GoMG3D	0.96	0.89	0.90	0.52	0.44	0.89	0.55	0.54	0.38
GoMTiS	0.90	0.81	0.88	0.53	0.58	0.83	0.55	0.53	0.56
GoMOKF	0.97	0.96	0.95	0.49	0.38	0.95	0.55	0.52	0.47
NThKF	0.99	0.97	0.77	0.32	0.41	0.93	0.33	0.31	0.37
NThBMJ	0.98	0.93	0.94	0.61	0.65	0.93	0.64	0.63	0.71
NThGF	0.98	0.87	0.89	0.48	0.48	0.90	0.54	0.54	0.44
NThG3D	0.84	0.87	0.43	0.22	0.06	0.80	0.25	0.24	0.05
NThTiS	0.87	0.79	0.73	0.32	0.22	0.78	0.30	0.29	0.19
NThOKF	0.92	0.92	0.63	0.28	0.27	0.93	0.30	0.26	0.27
MDMKF	0.89	0.86	0.47	0.27	0.12	0.84	0.31	0.32	0.09
MDMBMJ	0.99	0.97	0.94	0.69	0.79	0.96	0.72	0.71	0.74
MDMGF	0.98	0.91	0.87	0.47	0.45	0.95	0.55	0.54	0.34
MDMG3D	0.89	0.86	0.46	0.28	0.12	0.84	0.31	0.32	0.09
MDMTiS	0.90	0.84	0.68	0.33	0.34	0.85	0.34	0.38	0.27
MDMOKF	0.92	0.90	0.70	0.26	0.32	0.93	0.25	0.25	0.31
SBUKF	1.00	0.98	0.98	0.53	0.72	0.96	0.64	0.63	0.65
SBUBMJ	1.00	0.98	0.98	0.75	0.73	0.98	0.79	0.76	0.78
SBUGF	1.00	0.96	0.90	0.69	0.56	0.95	0.74	0.71	0.55
SBUG3D	0.90	0.89	0.54	0.35	0.19	0.85	0.38	0.36	0.15
SBUTiS	0.91	0.86	0.88	0.49	0.55	0.86	0.47	0.49	0.44
SBUOKF	1.00	0.79	0.85	0.63	0.67	0.95	0.69	0.66	0.63

Table A6. False Alarm Ratio (FAR).

Sch-Name	Kg.Sg. Soi	Pulau Manis	Paya Basar	PCCL Sg. Lembing	Rumah Pam	JKR Gamabng	Ldn Nada	Ldn Kuala Raman	JPS Negeri Pahang
KSKF	0.21	0.26	0.26	0.00	0.00	0.34	0.00	0.05	0.07
KSBMJ	0.20	0.25	0.24	0.05	0.08	0.32	0.00	0.24	0.11
KSGF	0.21	0.27	0.26	0.38	0.17	0.33	0.29	0.31	0.16
KSG3D	0.24	0.25	0.34	0.32	0.27	0.34	0.38	0.32	0.30
KSTiS	0.21	0.28	0.19	0.29	0.19	0.34	0.18	0.27	0.17
KSOKF	0.17	0.21	0.09	0.00	0.00	0.23	0.10	0.10	0.11
LinKF	0.25	0.29	0.30	0.92	0.42	0.38	0.64	0.78	0.53
LinBMJ	0.20	0.23	0.29	0.22	0.16	0.33	0.25	0.36	0.13
LinGF	0.16	0.24	0.20	0.22	0.11	0.29	0.16	0.19	0.14
LinG3D	0.19	0.29	0.35	0.31	0.17	0.35	0.39	0.39	0.17
LinTiS	0.21	0.29	0.22	0.14	0.23	0.36	0.14	0.22	0.22
LinOKF	0.17	0.26	0.25	0.21	0.38	0.31	0.24	0.28	0.42
WSM3KF	0.22	0.28	0.28	0.00	0.00	0.36	0.00	0.00	0.17
WSM3BMJ	0.18	0.22	0.21	0.24	0.15	0.32	0.25	0.24	0.06
WSM3GF	0.22	0.27	0.25	0.27	0.15	0.34	0.23	0.24	0.10
WSM3G3D	0.21	0.28	0.29	0.20	0.22	0.33	0.31	0.25	0.22
WSM3TiS	0.20	0.31	0.16	0.25	0.15	0.36	0.25	0.28	0.20
WSM3OKF	0.20	0.24	0.30	0.13	0.23	0.30	0.36	0.31	0.21
WSM6KF	0.23	0.27	0.31	1.00	0.15	0.35	0.83	0.71	0.46
WSM6BMJ	0.21	0.25	0.27	0.23	0.19	0.35	0.22	0.33	0.08
WSM6GF	0.15	0.26	0.17	0.26	0.09	0.30	0.19	0.20	0.15
WSM6G3D	0.26	0.29	0.32	0.52	0.25	0.36	0.43	0.38	0.18
WSM6TiS	0.24	0.30	0.24	0.24	0.21	0.36	0.33	0.35	0.22
WSM6OKF	0.21	0.23	0.20	0.15	0.32	0.33	0.17	0.24	0.22
GoMKF	0.24	0.27	0.31	0.25	0.20	0.35	0.25	0.30	0.18
GoMMBJ	0.19	0.27	0.28	0.24	0.10	0.34	0.24	0.33	0.12
GoMGF	0.22	0.27	0.22	0.23	0.24	0.34	0.21	0.24	0.25
GoMG3D	0.21	0.28	0.24	0.26	0.18	0.34	0.26	0.25	0.20
GoMTiS	0.21	0.30	0.27	0.25	0.13	0.36	0.27	0.25	0.18
GoMOKF	0.21	0.25	0.24	0.21	0.32	0.32	0.20	0.24	0.15
NThKF	0.22	0.26	0.26	0.40	0.17	0.34	0.38	0.43	0.22
NThBMJ	0.23	0.27	0.27	0.25	0.17	0.35	0.23	0.29	0.10
NThGF	0.18	0.28	0.27	0.24	0.16	0.32	0.23	0.24	0.19
NThG3D	0.17	0.27	0.35	0.35	0.00	0.33	0.35	0.36	0.00
NThTiS	0.20	0.30	0.19	0.14	0.00	0.36	0.16	0.19	0.00
NThOKF	0.15	0.24	0.25	0.37	0.21	0.31	0.33	0.41	0.21
MDMKF	0.21	0.27	0.34	0.22	0.21	0.33	0.35	0.28	0.25
MDMBMJ	0.23	0.26	0.29	0.25	0.13	0.34	0.26	0.29	0.16
MDMGF	0.21	0.27	0.24	0.20	0.14	0.29	0.18	0.13	0.13
MDMG3D	0.21	0.27	0.34	0.21	0.21	0.33	0.35	0.28	0.25
MDMTiS	0.22	0.29	0.25	0.09	0.11	0.34	0.23	0.20	0.19
MDMOKF	0.18	0.26	0.23	0.37	0.21	0.30	0.35	0.41	0.21
SBUKF	0.24	0.26	0.30	0.34	0.16	0.34	0.29	0.31	0.21
SBUBMJ	0.24	0.26	0.27	0.20	0.24	0.34	0.22	0.27	0.17
SBUGF	0.23	0.26	0.30	0.26	0.22	0.33	0.24	0.23	0.13
SBUG3D	0.23	0.27	0.35	0.27	0.14	0.34	0.31	0.30	0.29
SBUTiS	0.22	0.29	0.27	0.23	0.12	0.35	0.29	0.26	0.25
SBUOKF	0.22	0.28	0.26	0.29	0.20	0.34	0.27	0.31	0.22

Table A7. Bias (B).

Scheme Name	Kg.Sg. Soi	Pulau Manis	Paya Besar	PCCL Sg Lembing	Rumah Pam	JKR Gambang	Ladang Nada	Ladang Kuala Raman	JPS Negeri Pahang
KSKF	1.1	1.2	1.0	0.1	0.2	1.3	0.2	0.2	0.2
KSBMJ	1.1	1.1	1.0	0.2	0.3	1.2	0.2	0.3	0.2
KSGF	1.2	1.3	1.2	0.5	0.5	1.4	0.6	0.6	0.4
KSG3D	0.8	1.0	0.5	0.3	0.1	0.9	0.4	0.4	0.1
KSTiS	1.0	1.0	0.9	0.3	0.4	1.1	0.3	0.3	0.4
KSOKF	0.7	0.8	0.4	0.1	0.1	0.8	0.1	0.1	0.1
LinKF	1.1	1.2	0.8	0.1	0.1	1.2	0.1	0.1	0.2
LinBMJ	1.2	1.2	1.0	0.5	0.6	1.3	0.6	0.6	0.5
LinGF	1.1	1.1	1.1	0.6	0.5	1.2	0.7	0.7	0.4
LinG3D	1.0	1.1	0.7	0.3	0.1	1.2	0.4	0.3	0.1
LinTiS	1.1	1.1	1.0	0.3	0.3	1.2	0.3	0.4	0.3
LinOKF	0.9	1.0	0.7	0.2	0.1	1.1	0.2	0.2	0.1
WSM3KF	1.1	1.2	0.8	0.0	0.1	1.2	0.0	0.0	0.1
WSM3BMJ	1.1	1.1	0.9	0.4	0.4	1.1	0.4	0.4	0.4
WSM3GF	1.2	1.2	1.1	0.6	0.5	1.3	0.7	0.7	0.4
WSM3G3D	0.8	1.0	0.5	0.3	0.1	1.0	0.3	0.3	0.1
WSM3TiS	0.9	0.9	0.7	0.2	0.2	1.0	0.2	0.2	0.2
WSM3OKF	0.8	0.9	0.7	0.2	0.1	1.0	0.2	0.2	0.1
WSM6KF	1.2	1.3	1.1	0.1	0.2	1.4	0.1	0.1	0.2
WSM6BMJ	1.1	1.2	1.0	0.4	0.6	1.2	0.5	0.6	0.5
WSM6GF	1.2	1.2	1.1	0.7	0.6	1.3	0.7	0.7	0.4
WSM6G3D	1.1	1.1	0.7	0.3	0.1	1.2	0.4	0.4	0.2
WSM6TiS	1.2	1.1	1.0	0.3	0.3	1.2	0.3	0.3	0.3
WSM6OKF	1.2	1.3	0.8	0.4	0.2	1.2	0.4	0.4	0.3
GoMKF	1.3	1.3	1.4	1.2	1.2	1.4	1.3	1.3	1.2
GoMMBJ	1.2	1.3	1.1	0.6	0.6	1.4	0.7	0.7	0.5
GoMGF	1.3	1.3	1.2	0.8	0.8	1.4	0.9	0.9	0.6
GoMG3D	1.2	1.2	1.2	0.7	0.5	1.3	0.7	0.7	0.5
GoMTiS	1.1	1.2	1.2	0.7	0.7	1.3	0.8	0.7	0.7
GoMOKF	1.2	1.3	1.3	0.6	0.6	1.4	0.7	0.7	0.6
NThKF	1.3	1.3	1.0	0.5	0.5	1.4	0.5	0.5	0.5
NThBMJ	1.3	1.3	1.3	0.8	0.8	1.4	0.8	0.9	0.8
NThGF	1.2	1.2	1.2	0.6	0.6	1.3	0.7	0.7	0.5
NThG3D	1.0	1.2	0.7	0.3	0.1	1.2	0.4	0.4	0.1
NThTiS	1.1	1.1	0.9	0.4	0.2	1.2	0.4	0.4	0.2
NThOKF	1.1	1.2	0.8	0.4	0.3	1.3	0.4	0.4	0.3
MDMKF	1.1	1.2	0.7	0.3	0.1	1.3	0.5	0.4	0.1
MDMBMJ	1.3	1.3	1.3	0.9	0.9	1.5	1.0	1.0	0.9
MDMGF	1.2	1.2	1.1	0.6	0.5	1.3	0.7	0.6	0.4
MDMG3D	1.1	1.2	0.7	0.4	0.1	1.3	0.5	0.4	0.1
MDMTiS	1.2	1.2	0.9	0.4	0.4	1.3	0.4	0.5	0.3
MDMOKF	1.1	1.2	0.9	0.4	0.4	1.3	0.4	0.4	0.4
SBUKF	1.3	1.3	1.4	0.8	0.9	1.5	0.9	0.9	0.8
SBUBMJ	1.2	1.1	1.3	1.0	1.0	1.3	1.0	1.0	0.9
SBUGF	1.3	1.3	1.3	0.9	0.7	1.4	1.0	0.9	0.6
SBUG3D	1.2	1.2	0.8	0.5	0.2	1.3	0.6	0.5	0.2
SBUTiS	1.2	1.2	1.2	0.6	0.6	1.3	0.7	0.7	0.6
SBUOKF	1.3	1.1	1.1	0.9	0.8	1.4	0.9	1.0	0.8

Table A8. Rainfall event (mm): 21 December 2001 to 23 December 2001.

RF Stations	Observed	SBUBMJ	WSM6GF	LinGF	MDMBMJ	MDMGF
Kg Sg. Soi	351.9	462.9	82.7	140.5	371.1	109.8
Paya Besar	300.6	256.8	33.6	65.3	191.3	49.8
PCCL Sg. Lembing	498.0	504.9	42.2	79.6	509.8	94.4
Rumah Pam	601.9	958.4	45.0	169.3	640.6	128.7
Ladang Nada	470.7	587.4	44.8	86.5	548.2	120.3
Landan Kuala Raman	358.5	642.8	49.0	98.9	594.3	117.4
JPS Negeri Pahang	51.4	1014.4	39.1	171.1	616.3	124.5

Table A9. Rainfall event (mm): 29 December 2010 to 2 January 2011.

RF Stations	Observed	SBUBMJ	WSM6GF	LinGF	MDMBMJ	MDMGF
Kg Sg.Soi	223.8	186.9	90.9	77.5	114.9	93.4
Paya Besar	270.9	145.4	40.0	32.4	66.3	39.4
PCCL Sg. Lembing	248.6	168.6	189.9	159.7	98.7	110.2
Rumah Pam	268.1	215.1	137.7	66.3	112.2	105.5
JKR Gambang	177.5	213.2	71.5	87.9	101.5	104.6
Ladang Nada	208.1	198.6	163.0	181.0	92.1	147.1
Ladang Kuala Raman	192.2	233.4	186.8	209.0	88.3	188.7
JPS Negeri Pahang	363.4	249.6	70.5	42.9	139.7	51.3

Table A10. Rainfall event (mm): 26 January 2011 to 30 January 2011.

RF Stations	Observed	SBUBMJ	WSM6GF	LinGF	MDMBMJ	MDMGF
Kg Sg.Soi	121.3	118.4	69.532	74.883	101.117	66.762
Paya Besar	172.3	65.2	27.842	29.308	60.052	27.885
PCCL Sg. Lembing	185.9	140.7	188.121	228.847	139.354	240.554
Rumah Pam	161.7	143.8	52.979	40.589	110.148	71.243
Ladang Nada	159.3	141.0	117.419	204.061	148.404	219.386
Ladang Kuala Raman	151.4	133.0	101.591	168.675	144.688	128.793
JPS Negeri Pahang	177	147.7	37.689	23.598	103.042	42.075

Table A11. Rainfall event (mm): 26 March 2011 to 30 March 2011.

RF Stations	Observed	SBUBMJ	WSM6GF	LinGF	MDMBMJ	MDMGF
Kg Sg.Soi	46.9	62.2	237.147	266.113	94.69	230.476
PCCL Sg. Lembing	91.9	93.5	574.294	374.582	92.012	528.157
Rumah Pam	22.1	71.1	352.291	421.498	71.28	275.796
JKR Gambang	20.1	33.2	86.583	283.663	105.85	263.08
Ladang Nada	104.2	95.4	587.981	469.327	89.112	629.164
Ladang Kuala Raman	88.6	93.3	586.971	552.005	87.876	590.573
JPS Negeri Pahang	34.7	50.3	217.738	341.265	61.715	195.28

Table A12. Rainfall event (mm): 11 January 2012 to 13 January 2012.

RF Stations	Observed	SBUBMJ	WSM6GF	LinGF	MDMBMJ	MDMGF
Kg Sg.Soi	323.3	191.9	98.5	101.7	162.9	107.8
Paya Besar	280	90.0	45.7	46.0	76.6	50.4
PCCL Sg. Lembing	252.1	270.4	102.0	20.5	243.5	100.9
Rumah Pam	334.3	241.7	147.2	111.3	203.9	151.7
Ladang Nada	310.4	259.2	115.3	72.0	251.6	117.5
Ladang Kuala Raman	309.6	243.4	114.4	98.8	234.0	136.2
JPS Negeri Pahang	176.7	256.5	126.9	111.4	219.0	144.5

Table A13. Rainfall event (mm): 1 December 2013 to 5 December 2013.

RF Stations	Observed	SBUBMJ	WSM6GF	LinGF	MDMBMJ	MDMGF
JKR Gambang	592.8	287.3	351.9	439.6	274.2	263.1
Rumah Pam	1074.4	397.5	312.3	487.1	360.4	275.8
Kg. Sg. Soi	768.5	320.1	305.1	384.5	290.8	230.5
Ladng Nada	621.5	277.5	440.7	923.5	296.0	629.2

Table A14. Rainfall event (mm): 8 December 2016 to 12 December 2016.

RF Station	Observed	SBUBMJ	WSM6GF	LinGF	MDMBMJ	MDMGF
Kg. Sg.Soi	62.8	72.3	75.5	62.4	48.5	68.5
Paya Besar	60	74.1	32.8	27.1	30.1	30.2
PCCL Sg. Lembing	18.3	52.0	387.1	224.8	64.5	345.5
Rumah Pam	60.1	58.1	57.4	59.6	44.4	69.5
JKR Gambang	16.5	19.4	85.6	73.2	60.6	77.9
Ladang Nada	60.1	71.6	230.4	189.9	54.4	211.9
Ladang Kuala Raman	60.1	70.1	172.7	180.1	53.4	112.2
JPS Negeri Pahang	60	80.4	22.4	32.7	39.4	35.5

References

1. Bližňák, V.; Pokorná, L.; Rulfová, Z. Assessment of the Capability of Modern Reanalyses to Simulate Precipitation in Warm Months Using Adjusted Radar Precipitation. *J. Hydrol. Reg. Stud.* **2022**, *42*, 101121. [CrossRef]
2. Michaelides, S. Editorial for Special Issue "Remote Sensing of Precipitation". *Remote Sens.* **2019**, *11*, 389. [CrossRef]
3. Leta, O.T.; El-Kadi, A.I.; Dulai, H. Impact of Climate Change on Daily Streamflow and Its Extreme Values in Pacific Island Watersheds. *Sustainability* **2018**, *10*, 2057. [CrossRef]
4. Goncalves, M.L.R.; Zischg, J.; Rau, S.; Sitzmann, M.; Rauch, W.; Kleidorfer, M. Modeling the Effects of Introducing Low Impact Development in a Tropical City: A Case Study from Joinville, Brazil. *Sustainability* **2018**, *10*, 728. [CrossRef]
5. Coppola, E.; Giorgi, F. An Assessment of Temperature and Precipitation Change Projections over Italy from Recent Global and Regional Climate Model Simulations. *Int. J. Climatol. A J. R. Meteorol. Soc.* **2010**, *30*, 11–32. [CrossRef]
6. Figueroa, S.N.; Bonatti, J.P.; Kubota, P.Y.; Grell, G.A.; Morrison, H.; Barros, S.R.M.; Fernandez, J.P.R.; Ramirez, E.; Siqueira, L.; Luzia, G.; et al. The Brazilian Global Atmospheric Model (BAM): Performance for Tropical Rainfall Forecasting and Sensitivity to Convective Scheme and Horizontal Resolution. *Weather Forecast.* **2016**, *31*, 1547–1572. [CrossRef]
7. Lehtonen, I.; Ruosteenoja, K.; Jylhä, K. Projected Changes in European Extreme Precipitation Indices on the Basis of Global and Regional Climate Model Ensembles. *Int. J. Climatol.* **2014**, *34*, 1208–1222. [CrossRef]
8. Li, L.; Gochis, D.J.; Sobolowski, S.; Mesquita, M.D. Evaluating the Present Annual Water Budget of a Himalayan Headwater River Basin Using a High-resolution Atmosphere-hydrology Model. *J. Geophys. Res. Atmos.* **2017**, *122*, 4786–4807. [CrossRef]
9. Ratna, S.B.; Sikka, D.R.; Dalvi, M.; Ratnam, V.J. Dynamical Simulation of Indian Summer Monsoon Circulation, Rainfall and Its Interannual Variability Using a High Resolution Atmospheric General Circulation Model. *Int. J. Climatol.* **2011**, *31*, 1927–1942. [CrossRef]
10. Khansalari, S.; Ranjbar-Saadatabadi, A.; Fazel-Rastgar, F.; Raziei, T. Synoptic and Dynamic Analysis of a Flash Flood-Inducing Heavy Rainfall Event in Arid and Semi-Arid Central-Northern Iran and Its Simulation Using the WRF Model. *Dyn. Atmos. Oceans* **2021**, *93*, 101198. [CrossRef]
11. Prathipati, V.K.; Viswanadhapalli, Y.; Chennu, V.N.; Dasari, H.P. Evaluation of Weather Research and Forecasting Model Downscaled Rainfall and Its Variability over India. *Int. J. Climatol.* **2022**, *42*, 1418–1444. [CrossRef]
12. Srinivas, C.; Hariprasad, D.; Bhaskar Rao, D.; Anjaneyulu, Y.; Baskaran, R.; Venkatraman, B. Simulation of the Indian Summer Monsoon Regional Climate Using Advanced Research WRF Model. *Int. J. Climatol.* **2013**, *33*, 1195–1210. [CrossRef]
13. Liu, L.; Ma, Y.; Menenti, M.; Zhang, X.; Ma, W. Evaluation of WRF Modeling in Relation to Different Land Surface Schemes and Initial and Boundary Conditions: A Snow Event Simulation over the Tibetan Plateau. *J. Geophys. Res. Atmos.* **2019**, *124*, 209–226. [CrossRef]
14. Pegahfar, N.; Gharaylou, M.; Shoushtari, M.H. Assessing the Performance of the WRF Model Cumulus Parameterization Schemes for the Simulation of Five Heavy Rainfall Events over the Pol-Dokhtar, Iran during 1999–2019. *Nat. Hazards* **2022**, *112*, 253–279. [CrossRef]
15. Dasari, H.P.; Salgado, R.; Perdigao, J.; Challa, V.S. A Regional Climate Simulation Study Using WRF-ARW Model over Europe and Evaluation for Extreme Temperature Weather Events. *Int. J. Atmos. Sci.* **2014**, *2014*. [CrossRef]
16. Huang, D.; Gao, S. Impact of Different Reanalysis Data on WRF Dynamical Downscaling over China. *Atmos. Res.* **2018**, *200*, 25–35. [CrossRef]

17. Comin, A.N.; Justino, F.; Pezzi, L.; de Sousa Gurjão, C.D.; Shumacher, V.; Fernández, A.; Sutil, U.A. Extreme Rainfall Event in the Northeast Coast of Brazil: A Numerical Sensitivity Study. *Meteorol. Atmos. Phys.* **2021**, *133*, 141–162. [CrossRef]
18. Yang, Q.; Yu, Z.; Wei, J.; Yang, C.; Gu, H.; Xiao, M.; Shang, S.; Dong, N.; Gao, L.; Arnault, J.; et al. Performance of the WRF Model in Simulating Intense Precipitation Events over the Hanjiang River Basin, China—A Multi-Physics Ensemble Approach. *Atmos. Res.* **2021**, *248*, 105206. [CrossRef]
19. Grabowski, W.W.; Morrison, H.; Shima, S.-I.; Abade, G.C.; Dziekan, P.; Pawlowska, H. Modeling of Cloud Microphysics: Can We Do Better? *Bull. Am. Meteorol. Soc.* **2019**, *100*, 655–672. [CrossRef]
20. Wang, W. Forecasting Convection with a "Scale-Aware" Tiedtke Cumulus Parameterization Scheme at Kilometer Scales. *Weather Forecast.* **2022**, *37*, 1491–1507. [CrossRef]
21. Madhulatha, A.; Dudhia, J.; Park, R.; Rajeevan, M. Simulation of Latent Heating Rate From the Microphysical Process Associated With Mesoscale Convective System Over Korean Peninsula. *Earth Space Sci.* **2022**, *9*, e2022EA002419. [CrossRef]
22. Das, S.; Ashrit, R.; Iyengar, G.R.; Mohandas, S.; Das Gupta, M.; George, J.P.; Rajagopal, E.N.; Dutta, S.K. Skills of Different Mesoscale Models over Indian Region during Monsoon Season: Forecast Errors. *J. Earth Syst. Sci.* **2008**, *117*, 603–620. [CrossRef]
23. Pithani, P.; Ghude, S.D.; Prabhakaran, T.; Karipot, A.; Hazra, A.; Kulkarni, R.; Chowdhuri, S.; Resmi, E.; Konwar, M.; Murugavel, P.; et al. WRF Model Sensitivity to Choice of PBL and Microphysics Parameterization for an Advection Fog Event at Barkachha, Rural Site in the Indo-Gangetic Basin, India. *Theor. Appl. Climatol.* **2019**, *136*, 1099–1113. [CrossRef]
24. Song, H.-J.; Sohn, B.-J. An Evaluation of WRF Microphysics Schemes for Simulating the Warm-Type Heavy Rain over the Korean Peninsula. *Asia-Pac. J. Atmos. Sci.* **2018**, *54*, 225–236. [CrossRef]
25. Verma, S.; Panda, J.; Rath, S.S. Role of PBL and Microphysical Parameterizations during WRF Simulated Monsoonal Heavy Rainfall Episodes over Mumbai. *Pure Appl. Geophys.* **2021**, *178*, 3673–3702. [CrossRef]
26. Attada, R.; Dasari, H.P.; Kunchala, R.K.; Langodan, S.; Niranjan Kumar, K.; Knio, O.; Hoteit, I. Evaluating Cumulus Parameterization Schemes for the Simulation of Arabian Peninsula Winter Rainfall. *J. Hydrometeorol.* **2020**, *21*, 1089–1114. [CrossRef]
27. Musa, A.I.; Tsubo, M.; Ma, S.; Kurosaki, Y.; Ibaraki, Y.; Ali-Babiker, I.-E.A. Evaluation of WRF Cumulus Parameterization Schemes for the Hot Climate of Sudan Emphasizing Crop Growing Seasons. *Atmosphere* **2022**, *13*, 572. [CrossRef]
28. Constantinidou, K.; Hadjinicolaou, P.; Zittis, G.; Lelieveld, J. Performance of Land Surface Schemes in the WRF Model for Climate Simulations over the MENA-CORDEX Domain. *Earth Syst. Environ.* **2020**, *4*, 647–665. [CrossRef]
29. Srivastava, P.K.; Han, D.; Rico-Ramirez, M.A.; O'Neill, P.; Islam, T.; Gupta, M.; Dai, Q. Performance Evaluation of WRF-Noah Land Surface Model Estimated Soil Moisture for Hydrological Application: Synergistic Evaluation Using SMOS Retrieved Soil Moisture. *J. Hydrol.* **2015**, *529*, 200–212. [CrossRef]
30. Gómez, I.; Molina, S.; Galiana-Merino, J.J.; Estrela, M.J.; Caselles, V. Impact of Noah-LSM Parameterizations on WRF Mesoscale Simulations: Case Study of Prevailing Summer Atmospheric Conditions over a Typical Semi-Arid Region in Eastern Spain. *Sustainability* **2021**, *13*, 11399. [CrossRef]
31. Rai, D.; Pattnaik, S. Evaluation of WRF Planetary Boundary Layer Parameterization Schemes for Simulation of Monsoon Depressions over India. *Meteorol. Atmos. Phys.* **2019**, *131*, 1529–1548. [CrossRef]
32. Zeyaeyan, S.; Fattahi, E.; Ranjbar, A.; Azadi, M.; Vazifedoust, M. Evaluating the Effect of Physics Schemes in WRF Simulations of Summer Rainfall in North West Iran. *Climate* **2017**, *5*, 48. [CrossRef]
33. Lekhadiya, H.S.; Jana, R.K. Sensitivity of the WRF Model to the Parameterized Physical Process. In *Recent Advances in Intelligent Information Systems and Applied Mathematics*; Castillo, O., Jana, D.K., Giri, D., Ahmed, A., Eds.; Studies in Computational Intelligence; Springer International Publishing: Cham, Switzerland, 2020; Volume 863, pp. 170–181. ISBN 978-3-030-34151-0.
34. Ardie, W.A.; Sow, K.S.; Tangang, F.T.; Hussin, A.G.; Mahmud, M.; Juneng, L. The Performance of Different Cumulus Parameterization Schemes in Simulating the 2006/2007 Southern Peninsular Malaysia Heavy Rainfall Episodes. *J. Earth Syst. Sci.* **2012**, *121*, 317–327. [CrossRef]
35. Umer, Y.; Ettema, J.; Jetten, V.; Steeneveld, G.-J.; Ronda, R. Evaluation of the WRF Model to Simulate a High-Intensity Rainfall Event over Kampala, Uganda. *Water* **2021**, *13*, 873. [CrossRef]
36. Khan, M.M.A.; Shaari, N.A.B.; Bahar, A.M.A.; Baten, M.A.; Nazaruddin, D.B. Flood Impact Assessment in Kota Bharu, Malaysia: A Statistical Analysis. *World Appl. Sci. J.* **2014**, *32*, 626–634.
37. Jamaluddin, A.F.; Kamal, M.I.M.; Abdullah, M.H.; Marodzi, A.N. Comparison between Satellite-Derived Rainfall and Rain Gauge Observation over Peninsular Malaysia. *Sains Malays.* **2022**, *51*, 67–81. [CrossRef]
38. Akasah, Z.A.; Doraisamy, S.V. 2014 Malaysia Flood: Impacts & Factors Contributing towards the Restoration of Damages. *J. Sci. Res. Dev.* **2015**, *2*, 53–59.
39. Romali, N.S.; Sulaiman, M.; Khushren, S.; Yusop, Z.; Ismail, Z. Flood Damage Assessment: A Review of Flood Stage–Damage Function Curve. *ISFRAM 2014* **2015**, 147–159. [CrossRef]
40. Romali, N.S.; Yusop, Z.; Sulaiman, M.; Ismail, Z. Flood Risk Assessment: A Review of Flood Damage Estimation Model for Malaysia. *J. Teknol.* **2018**, *80*. [CrossRef]
41. Safiah Yusmah, M.Y.; Bracken, L.J.; Sahdan, Z.; Norhaslina, H.; Melasutra, M.D.; Ghaffarianhoseini, A.; Sumiliana, S.; Shereen Farisha, A.S. Understanding Urban Flood Vulnerability and Resilience: A Case Study of Kuantan, Pahang, Malaysia. *Nat. Hazards* **2020**, *101*, 551–571. [CrossRef]
42. Jamaludin, M.H.; Jaafar, S.; Chuah, B.K.; Abdullah, Z. *Flood: Kuantan Town Centre Almost Paralysed, 37,100 Evacuated in 4 States*; The News Straits Times Press: Kuala Lumpur, Malaysia, 2013.

43. Shah, S.M.H.; Mustaffa, Z.; Yusof, K.W. Disasters Worldwide and Floods in the Malaysian Region: A Brief Review. *Indian J. Sci. Technol.* **2017**, *10*, 1–9. [CrossRef]
44. Zaidi, S.M.; Gisen, J.I.A. Evaluation of Weather Research and Forecasting (WRF) Microphysics Single Moment Class-3 and Class-6 in Precipitation Forecast. *MATEC Web Conf.* **2018**, *150*, 03007. [CrossRef]
45. Chai, T.; Draxler, R.R. Root Mean Square Error (RMSE) or Mean Absolute Error (MAE)?—Arguments against Avoiding RMSE in the Literature. *Geosci. Model Dev.* **2014**, *7*, 1247–1250. [CrossRef]
46. Zelelew, D.; Melesse, A. Applicability of a Spatially Semi-Distributed Hydrological Model for Watershed Scale Runoff Estimation in Northwest Ethiopia. *Water* **2018**, *10*, 923. [CrossRef]
47. Schwartz, C.S. A Comparison of Methods Used to Populate Neighborhood-Based Contingency Tables for High-Resolution Forecast Verification. *Weather Forecast.* **2017**, *32*, 733–741. [CrossRef]
48. Opijah, F.J.; Mutemi, J.N.; Ogallo, L.A. Seasonal Climate Predictability over Kenya Using the Regional Spectral Model. *J. Meteorol. Relat. Sci.* **2017**, *10*, 12–24. [CrossRef]
49. Racoma, B.; Crisologo, I.; David, C. Accumulation-Based Advection Field for Rainfall Nowcasting. *J. Philipp. Geosci. Remote Sens. Soc.* **2015**, *1*, 21–26.
50. Salimun, E.; Tangang, F.; Juneng, L. Simulation of Heavy Precipitation Episode over Eastern Peninsular Malaysia Using MM5: Sensitivity to Cumulus Parameterization Schemes. *Meteorol. Atmos. Phys.* **2010**, *107*, 33–49. [CrossRef]
51. Sikder, S.; Hossain, F. Assessment of the Weather Research and Forecasting Model Generalized Parameterization Schemes for Advancement of Precipitation Forecasting in Monsoon-driven River Basins. *J. Adv. Model. Earth Syst.* **2016**, *8*, 1210–1228. [CrossRef]
52. Madhulatha, A.; Rajeevan, M. Impact of Different Parameterization Schemes on Simulation of Mesoscale Convective System over South-East India. *Meteorol. Atmos. Phys.* **2018**, *130*, 49–65. [CrossRef]
53. Morrison, H.; Milbrandt, J.A.; Bryan, G.H.; Ikeda, K.; Tessendorf, S.A.; Thompson, G. Parameterization of Cloud Microphysics Based on the Prediction of Bulk Ice Particle Properties. Part II: Case Study Comparisons with Observations and Other Schemes. *J. Atmos. Sci.* **2015**, *72*, 312–339. [CrossRef]
54. Kuo, C.-C.; Gan, T.Y. Estimation of Precipitation and Air Temperature over Western Canada Using a Regional Climate Model. *Int. J. Climatol.* **2018**, *38*, 5125–5135. [CrossRef]
55. Reshmi Mohan, P.; Srinivas, C.V.; Yesubabu, V.; Baskaran, R.; Venkatraman, B. Simulation of a Heavy Rainfall Event over Chennai in Southeast India Using WRF: Sensitivity to Microphysics Parameterization. *Atmos. Res.* **2018**, *210*, 83–99. [CrossRef]
56. Toride, K.; Cawthorne, D.L.; Ishida, K.; Kavvas, M.L.; Anderson, M.L. Long-Term Trend Analysis on Total and Extreme Precipitation over Shasta Dam Watershed. *Sci. Total Environ.* **2018**, *626*, 244–254. [CrossRef]
57. Haghroosta, T.; Ismail, W.R.; Ghafarian, P.; Barekati, S.M. The Efficiency of the Weather Research and Forecasting (WRF) Model for Simulating Typhoons. *Nat. Hazards Earth Syst. Sci.* **2014**, *14*, 2179–2187. [CrossRef]
58. Chawla, I.; Osuri, K.K.; Mujumdar, P.P.; Niyogi, D. Assessment of the Weather Research and Forecasting (WRF) Model for Simulation of Extreme Rainfall Events in the Upper Ganga Basin. *Hydrol. Earth Syst. Sci.* **2018**, *22*, 1095–1117. [CrossRef]
59. Remesan, R.; Bellerby, T.; Holman, I.; Frostick, L. WRF Model Sensitivity to Choice of Parameterization: A Study of the 'York Flood 1999'. *Theor. Appl. Climatol.* **2015**, *122*, 229–247. [CrossRef]